Cell Reports

Article

Adenosine signaling in glia modulates metabolic state-dependent behavior in *Drosophila*

Graphical abstract

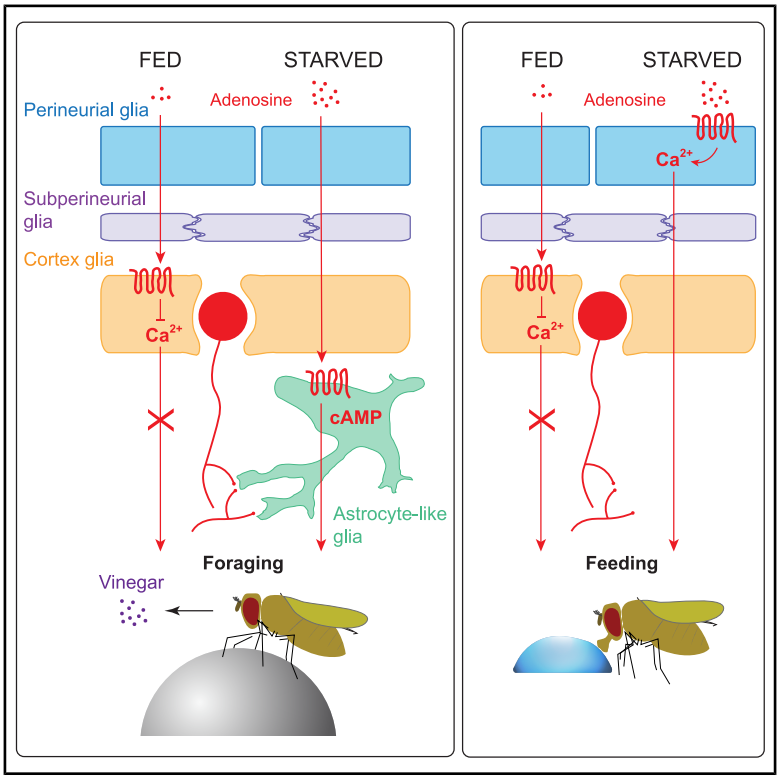

Highlights

- Adenosine signaling in specific glia subtypes modulates feeding-state-dependent behavior
- Blood-brain-barrier glia and astrocytes promote feeding and foraging, respectively
- Cortex glia suppress feeding and foraging
- Glia adenosine receptors regulate dopaminergic neuron activity

Authors

Jean-François De Backer, Thomas Karges, Julia Papst, ..., Yanjun Xu, Cristina García-Cáceres, Ilona C. Grunwald Kadow

Correspondence

ilona.grunwald@uni-bonn.de

In brief

De Backer et al. dissect the roles of adenosine signaling in glia subtypes in the fly nervous system and their relationship to feeding-state-dependent behavior. Their results provide a potentially conserved mechanism used by animals to sense their internal energetic state and adjust their behavior accordingly.

De Backer et al., 2025, Cell Reports *44*, 115765
June 24, 2025
https://doi.org/10.1016/j.celrep.2025.115765

CellPress

Cell Reports

CellPress
OPEN ACCESS

Article

Adenosine signaling in glia modulates metabolic state-dependent behavior in *Drosophila*

Jean-François De Backer,[1] Thomas Karges,[1] Julia Papst,[1] Zeynep Nigar Pınar,[1] Cristina Coman,[2] Robert Ahrends,[2] Yanjun Xu,[3,4] Cristina García-Cáceres,[3,4] and Ilona C. Grunwald Kadow[1,5,*]

[1]Institute of Physiology II, Faculty of Medicine, University of Bonn, Bonn, Germany
[2]Institute of Analytical Chemistry, University of Vienna, Vienna, Austria
[3]Institute of Diabetes and Obesity, Helmholtz Diabetes Center, Helmholtz Zentrum München, Neuherberg, Germany
[4]German Center for Diabetes Research (DZD), Neuherberg, Germany
[5]Lead contact
*Correspondence: ilona.grunwald@uni-bonn.de
https://doi.org/10.1016/j.celrep.2025.115765

SUMMARY

An animal's metabolic state strongly influences its behavior. Hungry animals prioritize food-seeking and feeding behaviors, while sated animals suppress these behaviors to engage in other activities. Additionally, neuronal activity and synaptic transmission are among the most energy-expensive processes. However, neurons do not uptake nutrients from the circulation. Instead, glia fulfill this highly evolutionarily conserved function in addition to modulating neuronal activity and behavior. However, how different glia subtypes sense metabolic state and modulate behavior is incompletely understood. Here, we unravel two types of glia-mediated modulation of metabolic-state-dependent behavior. In food-deprived flies, astrocyte-like and perineurial glia promote foraging and feeding, respectively, while cortex glia suppress these behaviors. We further show that adenosine and adenosine receptors modulate intracellular calcium levels in these glia subtypes, which ultimately controls behavior. This study reveals a mechanism of how different glia subtypes sense an animal's metabolic state and modulate its behavior accordingly.

INTRODUCTION

Most animals live in dynamic environments where nutrient availability fluctuates, requiring behavioral and metabolic adaptation. To prepare for periods of food scarcity, animals mobilize internal energy stores and prioritize behaviors such as foraging.[1–3] However, these behaviors are themselves energy demanding and must therefore be tightly regulated and repressed when the animal reaches satiation. While neuronal processing is known to be modulated by metabolic state,[4,5] the role of glia—the other major cell type in the nervous system—in regulating metabolism-related behavior remains underexplored.

Glia, long known as support cells for neurons, respond to neurotransmitters via changes in internal calcium[6] and modulate neuronal activity through various mechanisms such as neurotransmitter turnover, potassium buffering, and release of signaling molecules often referred to as gliotransmitters.[7,8] This bidirectional neuron-glial communication influences diverse behaviors across species.[8] In the context of metabolic state and obesity, astrocytes in the hypothalamus influence neuronal activity and food intake in mice.[9–12] Given their widespread distribution as well as their extended arborization and nets, glial cells are well positioned for broadcasting essential physiological states globally across the nervous system.[8]

Similar to in mammals, glia in insects comprise different subtypes distributed according to their function within the central nervous system (CNS).[13–15] Cortex glia (CG) tightly embed neuronal somas, which are, contrary to vertebrates, located at the surface of the fly's brain. There, CG modulate neuronal excitability[16,17] and provide necessary nutrients for neurons to sustain memory formation.[18] From the surface, flies' monopolar neurons send neurites that further differentiate into axons and dendrites, forming the neuropil. Within the neuropil, astrocyte-like glia (ALG) interact with synapses, while ensheathing glia (ENG) interact with neurites and form internal barriers separating neuropil compartments. Several studies have shown that ALG are involved in the modulation of different behaviors in flies, including sleep homeostasis, chemotaxis, or drinking,[19–21] while ENG participate in the transmission of negative stimuli during memory formation and are involved in sleep homeostasis.[22,23]

Two further glial types—the perineurial glia (PNG) and subperineurial glia (SPN)—form the fly's hemolymph-brain barrier (HBB), akin to the mammalian blood-brain barrier (BBB).[24,25] SPN cells form septate junctions regulating molecular flow into the CNS, while PNG cells assist in nutrient transport and CNS energy supply.[26,27]

Given their position at the interface between circulation and neurons, glia and the BBB have recently been proposed to detect nutrient availability in the blood or the hemolymph and to transmit this information to the rest of the nervous system.[11,28–32] Although the mechanisms enabling glia to sense

metabolic state are currently unknown, we hypothesized that ATP, the energetic unit of living organisms, could be a good candidate to bridge metabolic sensing and adaptive behavior in response to high energy demand or deprivation. In addition to being released and detected in the nervous system by both neurons and glia, ATP can be hydrolyzed into adenosine.[33] Among its many functions,[34–38] extracellular adenosine contributes to energetic metabolism by signaling cellular energy demand in different tissues.[39] In the nervous system, lower concentrations of ATP/adenosine were suggested to promote more demanding cognitive tasks when energy is available and higher concentrations to encourage behaviors related to food seeking.[32] According to this model, purinergic signaling would provide information to the brain about the organism's low energetic context in order to prioritize food search and energy saving through lowering demanding cognitive activity and resting. However, this appealing model remains to be formally demonstrated.

In this study, we provide evidence supporting this model. We show that adenosine accumulates in starved flies and is detected by various glial subpopulations, including HBB-forming glia. Adenosine signaling alters glial calcium responses depending on metabolic state and modulates behavior to promote food seeking and feeding. These findings provide a new mechanism used by flies, and potentially other animals, to adapt their behavior in response to their systemic energy levels.

RESULTS

Circulating adenosine modulates feeding behavior in starved flies

Previous studies have shown that adenosine signaling regulates carbohydrate metabolism in fly larvae: mutants with elevated systemic adenosine exhibit impaired glycogen storage and increased circulating glucose.[40] Additionally, adenosine is produced during infections in response to the heightened nutrient demands of active immune cells.[41,42] We therefore hypothesized that adenosine acts as a systemic signal of energy deprivation in starved flies. To test this, we measured adenosine levels in starved flies using mass spectrometry and found a significant increase after 24 h of starvation compared to fed controls (Figure 1A), suggesting that food deprivation leads to an increase in systemic adenosine levels.

We next assessed whether elevated adenosine impacts feeding behavior by mimicking starvation in fed flies. Wild-type flies were fed standard food supplemented with the chemically stable adenosine receptor (AdoR) agonist 2-chloroadenosine (2 mM).[43] To analyze the impact of this manipulation on feeding behavior, we used the FlyPAD feeding assay[44] (Figures 1B and S1A). Interestingly, we found that systemic and chronic AdoR activation significantly increased the number of sips taken on 10% sucrose in fed flies, mimicking starved flies' behavior (Figure 1C). The FlyPAD assay also enables detailed feeding pattern analysis.[44] Similar to rodents, flies feed in activity bouts—when the animal visits the food source—subdivided into bursts of sips[45] (Figure 1B). As expected, 24-h-starved wild-type flies showed increased sip duration, burst number and duration, and more activity bouts compared to fed flies[44] (Figures S1B–S1G). Similarly, 2-chloroadenosine-fed flies visited sucrose drops more frequently and displayed longer and more frequent feeding bursts (Figures S1H–S1M).

In addition to the FlyPAD, we used an olfactory-driven spherical treadmill paradigm that we previously developed as a proxy for metabolic-state-dependent persistence in foraging behavior[46] (Figure 1D). In brief, we have shown that hungry flies persistently track vinegar odor—a food-predicting cue—with increasing effort over ten trials in the absence of food reward, while fed flies do not. Remarkably, feeding flies with 2-chloroadenosine prior to the experiment induced a starvation-like state: fed flies track the successive vinegar-odor stimuli more persistently and more quickly (Figures 1E and 1F).

We then asked whether a state of perceived hunger could be induced by enhancing endogenous adenosine production. To do this, we reduced the expression of the adenosine deaminase growth factor A (AdgfA), an enzyme that converts adenosine into inactive inosine. Mutant flies for this enzyme have previously been shown to present an increase in adenosine levels.[40,47,48] We reduced *AdgfA* expression by knockdown via RNA interference (RNAi) in hemocytes, in which AdgfA promotes the mobilization of internal energy stores,[40–42,49] as well as in the fat body, where the enzyme is not expressed, as a control. Interestingly, hemocyte-specific *AdgfA* knockdown flies took about twice as many sips as controls (Figure 1G) and were less resistant to starvation, consistent with energy wasting[40] (Figure S1N). In 24-h-starved flies, *AdgfA* knockdown further increased sip duration, feeding-burst frequency and duration, and activity bouts (Figures S1O–S1T), suggesting that peripheral production of high levels of circulating adenosine promotes feeding in starved flies.

We next examined whether adenosine produced in the CNS also modulates feeding. The fly genome encodes multiple Adgf isoforms.[47] By analyzing previously published single-cell transcriptomic sequencing data using the SCope online tool, we found that *AdgfC* and *AdgfD* are likely expressed in the adult fly brain, mostly in glia.[50] We therefore knocked down *AdgfC* and *AdgfD* by expressing RNAi under the control of the pan-glia genetic driver Repo-Gal4. As a control, we also expressed the RNAi against *AdgfA*, since the expression of this isoform has not been reported in the fly brain. None of these manipulations affected feeding (Figure 1H).

Taken together, these results suggest that increased levels of adenosine circulating in the hemolymph are responsible for modulating feeding-state-dependent behavior in response to food deprivation.

Adenosine signaling in the CNS is necessary for feeding-state-dependent behavior

Having found that adenosine modulates feeding behavior, we next sought to identify the signaling mechanisms and cell types involved. Unlike mammals, flies likely rely on a single G-protein-coupled AdoR.[51] Transcriptomic data show that *AdoR* is predominantly expressed in glial cells, with some neuronal expression.[50] To determine where AdoR is required for metabolic-state-dependent behavior, we knocked down *AdoR* in neurons and glia, respectively.

AdoR knockdown in neurons led to increased sucrose consumption in 24-h-starved flies (Figure 2A). Interestingly, *AdoR* seems to be expressed in dopaminergic neurons (DANs) and

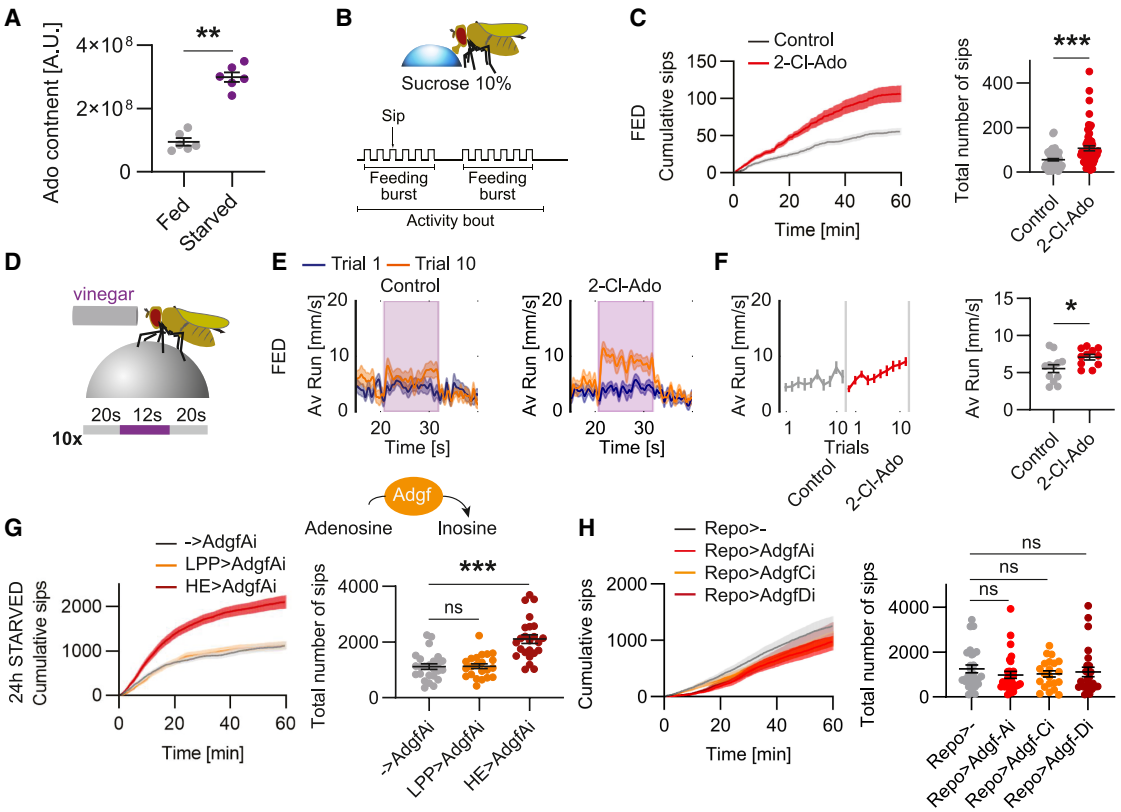

Figure 1. Extracellular adenosine is increased in food-deprived flies and promotes feeding and food-odor tracking behavior

(A) Adenosine content in fed vs. 24-h-starved CS flies (n = 6/6 replicates; 10 flies/replicate; Mann-Whitney U test, p = 0.0022).

(B) FlyPAD feeding assay. Single freely moving flies were feeding on agarose drops containing 10% sucrose for 1 h. Feeding behavior was assessed by both the number of sips and the feeding activity pattern.

(C) Cumulative number of sips (mean ± SEM) and total number of sips taken on 10% sucrose drops in fed wild-type flies kept for 5 days on standard fly food supplemented with the AdoR agonist 2-chloroadenosine (2-Cl-Ado; 2 mM; n = 57/57; Mann-Whitney U test, $p < 0.0001$).

(D) Odor-tracking paradigm. A single tethered fly is freely walking on an air floating ball and stimulated for 12 s with vinegar odor. This stimulation protocol is repeated over ten trials.

(E) Averaged forward running speed (±SEM) in fed flies kept for 5 days on standard fly food supplemented with 1.65 mM 2-Cl-Ado.

(F) Running speed during odor exposure (mean ± SEM; n = 10/12/12; 2-way repeated-measures [RM] ANOVA, p(groups) = 0.0282; p(trials) = 0.0034; p(interaction) = 0.55). The scatterplot displays the averaged running speed over the ten trials (unpaired t test, p = 0.0282).

(G) In the extracellular space, adenosine is degraded into inactive inosine by adenosine deaminases (Adgf). Cumulative number of sips (mean ± SEM) and total number of sips on 10% sucrose drops in 24-h-starved control flies (−>AdgfAi) or upon knockdown of AdgfA in the fat body (LPP>AdgfAi) or hemocytes (HE>AdgfAi; n = 25/22/24; Welch's one-way ANOVA, $p < 0.0001$).

(H) Cumulative number of sips (mean ± SEM) and total number of sips taken on 10% sucrose drops in 24-h-starved control flies (Repo>−) or upon knockdown of the different Adgf isoforms in glia (Repo>AdgfAi, -Ci, and -Di; n = 27/29/21/25; Kruskal-Wallis test p = 0.48).

Scatterplots display individual data points, as well as the mean ± SEM for each group. Pairwise comparisons: ns, non-significant ($p > 0.05$); *$p < 0.05$; **$p < 0.01$; ***$p < 0.001$. See also Figure S1.

octopaminergic neurons (OANs),[50] both implicated in state-dependent behaviors.[5,46] Targeted *AdoR* knockdown in these populations revealed that only flies deficient for *AdoR* in DANs consumed more sucrose than controls (Figures S2A–S2G), implicating that AdoR in DANs contributes to feeding regulation.

In contrast, glial-specific *AdoR* knockdown resulted in significantly reduced sucrose intake (Figure 2B). Feeding-structure analysis showed reductions in sip duration, food-source visit frequency, and feeding-burst duration and frequency (Figures S2H–S2M). To exclude developmental effects, we restricted AdoR-RNAi expression to adults using the RU486-inducible Gene-Switch system[52] and observed similarly reduced sucrose intake (Figures 2C and 2D). These findings suggest that systemic adenosine stimulates feeding via AdoR signaling in glia during starvation.

We also examined AdoR's role in food-odor tracking. Here, only glial—but not neuronal—*AdoR* knockdown in starved flies reduced forward running speed toward vinegar odor without affecting baseline locomotion, consistent with previous findings[53] (Figures 2E, 2F, and S2N), indicating reduced foraging persistence. This result was confirmed with a separate RNAi line (Figures S3A and S3B) and adult-restricted expression using the temperature-sensitive TARGET system,[54] which produced similar tracking deficits (Figures S3C–S3F).

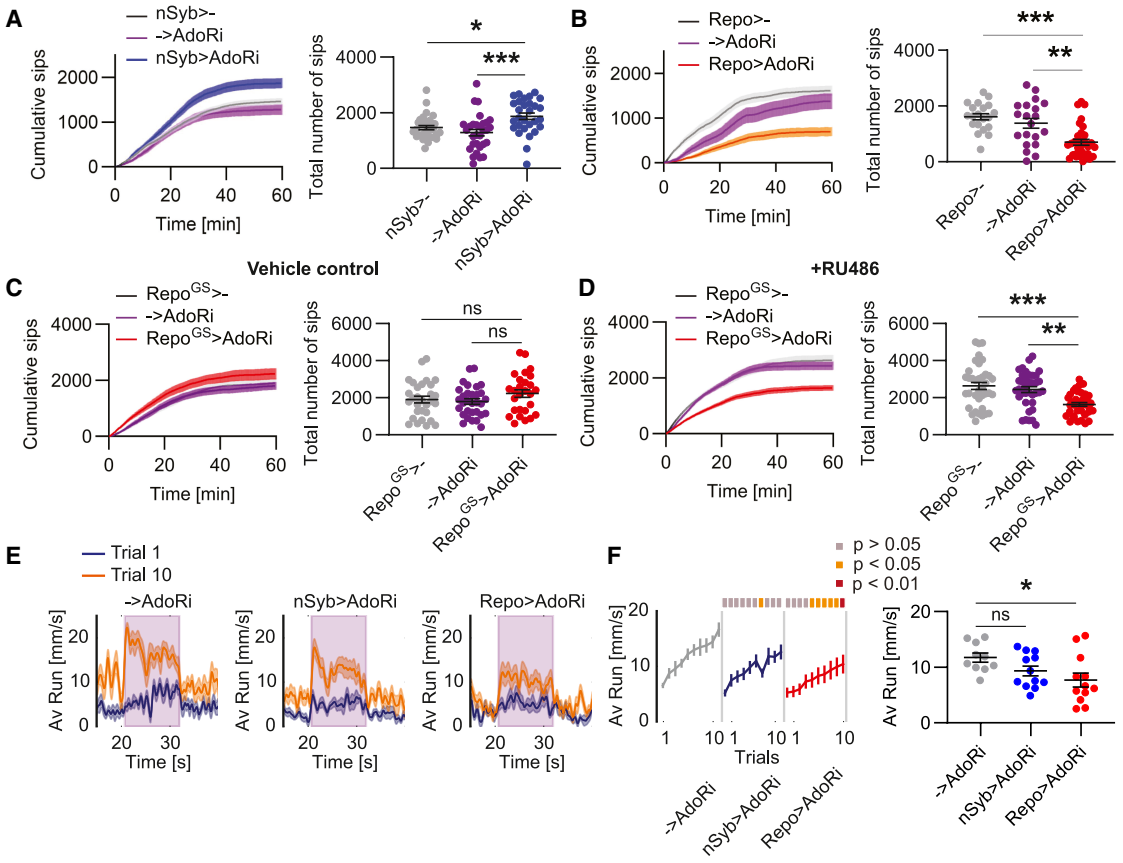

Figure 2. Adenosine signaling in glia is necessary for feeding-state-dependent behavior

(A) Cumulative number of sips (mean ± SEM) and total number of sips on 10% sucrose drops in 24-h-starved control flies (nSyb>– and –>AdoRi) or upon knockdown of AdoR in neurons (nSyb>AdoRi; n = 32/30/29; Kruskal-Wallis test, p = 0.0006).

(B) Cumulative number of sips (mean ± SEM) and total number of sips on 10% sucrose drops in 24-h-starved control flies (Repo>– and –>AdoRi) or upon knockdown of AdoR in glia (Repo>AdoRi; n = 20/20/32; Kruskal-Wallis test, $p < 0.0001$).

(C and D) Temporal restriction of knockdown of AdoR in glia using the Gene-Switch system. (C) Cumulative number of sips (mean ± SEM) and total number of sips on 10% sucrose drops in uninduced 24-h-starved flies (n = 27/31/30; one-way ANOVA, p = 0.21). (D) Cumulative number of sips (mean ± SEM) and total number of sips on 10% sucrose drops in 24-h-starved flies, after induction of Gal4 expression using RU486 (n = 37/37/37; Welch's one-way ANOVA, $p < 0.0001$).

(E) Averaged forward running speed (±SEM) in 24-h-starved control (–>AdoRi) flies or upon knockdown of AdoR in neurons (nSyb>AdoRi) and glia (Repo>AdoRi), respectively.

(F) Running speed during odor exposure (mean ± SEM; n = 10/12/12; 2-way RM ANOVA, p(groups) = 0.0366; p(trials) < 0.0001; p(interaction) = 0.40). Sidak's post hoc trial-to-trial comparisons are depicted on the top of the graphs as color-coded boxes (gray, $p > 0.05$; orange, $p < 0.05$; red, $p < 0.01$). The scatterplot displays the averaged running speed over the ten trials (one-way ANOVA, p = 0.0366).

Scatterplots display individual data points, as well as the mean ± SEM for each group. Post hoc pairwise comparisons: ns, non-significant; *$p < 0.05$; **$p < 0.01$; ***$p < 0.001$. See also Figures S2 and S3.

Overall, these data show that glial AdoR is necessary for both feeding and food-odor tracking in starved flies.

Adenosine signaling in specific glia subpopulations differentially modulates behavior

To further dissect the role of adenosine signaling in the different glia subpopulations with different positions and functions in the nervous system, we used subtype-specific driver lines[14] (Figure 3A).

Knocking down *AdoR* in PNG significantly reduced sip counts in 24-h-starved flies (Figure 3B), correlated with shorter activity bouts and feeding bursts, while activity bout and burst numbers were unchanged (Figures S4C–S4F). However, longer-term feeding behavior remained unaffected (Figure S4G), suggesting that other physiological mechanisms can compensate for the initial deficit. Consistent with this observation, these flies survived starvation for more than 60 h, suggesting that their long-term feeding behavior and nutrient storage is not affected (Figure S4H).

In contrast, *AdoR* knockdown in SPN did not alter total sip count (Figure 3B) but did reduce sip frequency and increase food-source visits (Figures S4B and S4C). These changes were balanced by shorter feeding bouts and bursts, yielding unchanged food intake (Figures S4D and S4F). Knocking down *AdoR* in ALG or ENG had no effect on feeding (Figures 3C and 3D). As PNG-specific knockdown mimicked the pan-glial

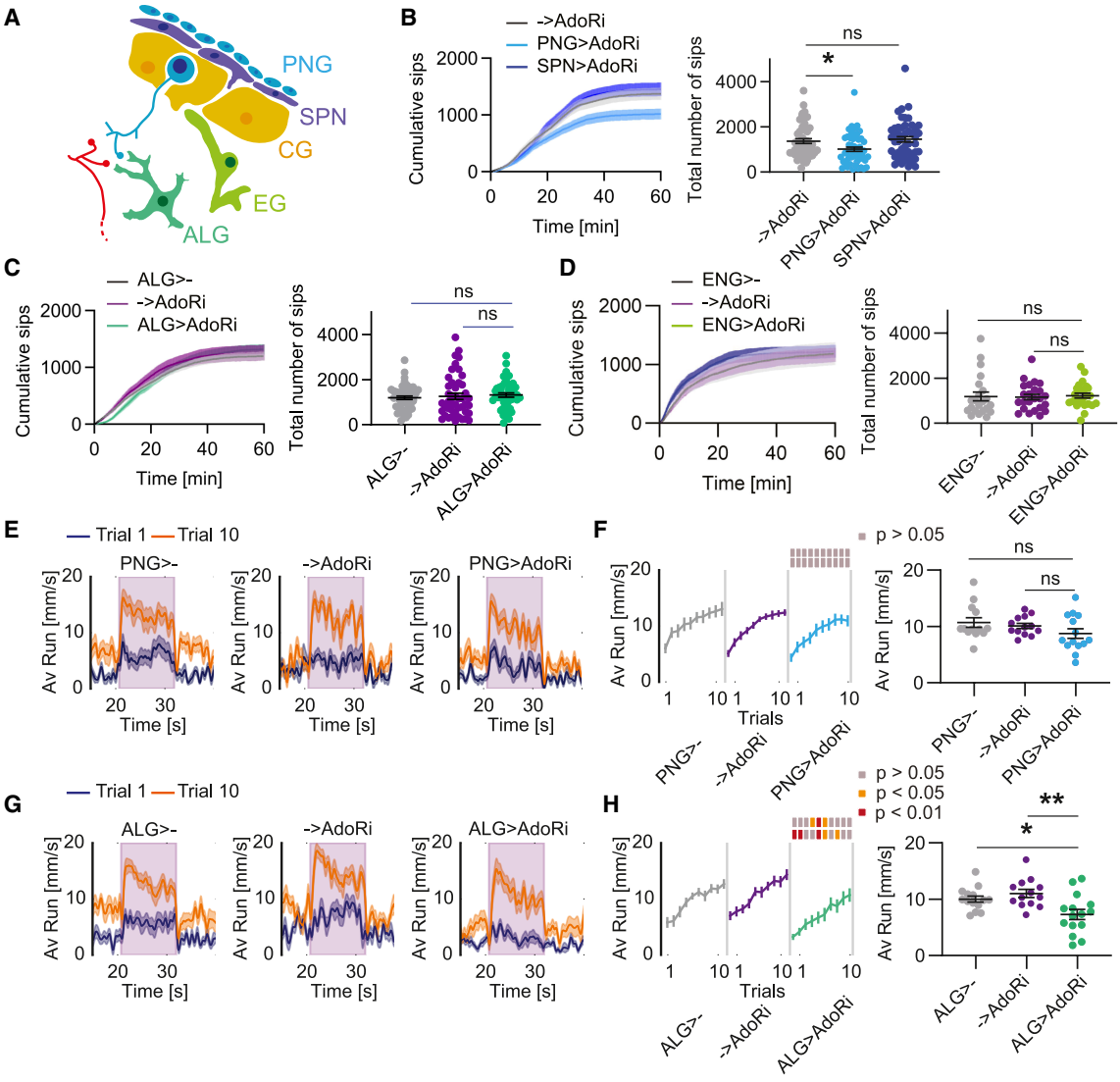

Figure 3. Adenosine signaling in perineurial and astrocyte-like glia subpopulations differentially affects feeding and food-odor tracking behavior

(A) Anatomical location of the different glia subpopulations in the fly CNS. PNG, perineurial glia; SPN, subperineurial glia; CG, cortex glia; ALG, astrocyte-like glia; ENG, ensheathing glia.

(B) Cumulative number of sips (mean ± SEM) and total number of sips on 10% sucrose drops in 24-h-starved control flies (−>AdoRi) or upon knockdown of AdoR in PNG (PNG>AdoRi) and SPN (SPN>AdoRi), respectively (n = 49/51/48; Kruskal-Wallis test, p = 0.0096).

(C) Cumulative number of sips (mean ± SEM) and total number of sips on 10% sucrose drops in 24-h-starved control flies (ALG>− and −>AdoRi) or upon knockdown of AdoR in ALG (ALG>AdoRi; n = 47/45/46; Kruskal-Wallis test, p = 0.39).

(D) Cumulative number of sips (mean ± SEM) and total number of sips on 10% sucrose drops in 24-h-starved control flies (ENG>− and −>AdoRi) or upon knockdown of AdoR in ENG (ENG>AdoRi; n = 22/24/24; Kruskal-Wallis test, p = 0.51).

(E) Averaged forward running speed (±SEM) in 24-h-starved control flies (PNG>− and −>AdoRi) or upon knockdown of AdoR in PNG (PNG>AdoRi).

(F) Running speed during odor exposure (mean ± SEM; n = 13/13/14; 2-way RM ANOVA, p(groups) = 0.19; p(trials) < 0.0001; p(interaction) = 0.99). The scatterplot displays the averaged running speed over the ten trials (one-way ANOVA, p = 0.19).

(G) Averaged forward running speed (±SEM) in 24-h control flies (ALG>− and −>AdoRi) or upon knockdown of AdoR in ALG (ALG>AdoRi).

(H) Running speed during odor exposure (mean ± SEM; n = 14/13/15; 2-way RM ANOVA, p(groups) = 0.0030; p(trials) < 0.0001; p(interaction) = 0.80). The scatterplot displays the averaged running speed over the ten trials (one-way ANOVA, p = 0.0030).

For food-odor tracking behavior experiments, Sidak's post hoc trial-to-trial comparisons are depicted on the top of the graphs as color-coded boxes (gray, $p > 0.05$; orange, $p < 0.05$; red, $p < 0.01$). Scatterplots display individual data points as well as the mean ± SEM for each group. Post hoc pairwise comparisons: ns, non-significant; *$p < 0.05$; **$p < 0.01$; ***$p < 0.001$. See also Figure S4.

phenotype, we concluded that AdoR in PNG is essential for starvation-induced feeding behavior.

Interestingly, PNG-specific *AdoR* knockdown did not impair food-odor tracking (Figures 3E and 3F). Neither SPN nor ENG knockdown affected vinegar tracking (Figures S4I–S4L). However, ALG-specific knockdown significantly reduced forward running speed in starved flies (Figures 3G and 3H), a result confirmed with a second RNAi line (Figures S4M and S4N). Innate vinegar attraction was intact (Figures S4O and S4P), and starvation survival was unaffected (Figure S4Q), indicating a specific deficit in persistent odor tracking rather than sensory or survival impairment.

In summary, AdoR is required in distinct glial subtypes for specific behaviors in starved flies: PNG AdoR promotes feeding, while ALG AdoR supports persistent food-odor tracking.

Adenosine signaling in cortex glia inhibits feeding-state-dependent behaviors

We have shown that AdoR signaling promotes foraging and feeding through distinct glial subtypes in response to increased adenosine levels in hungry flies. While *AdoR* knockdown in PNG and ALG replicated different aspects of pan-glial knockdown, knockdown in CG had an opposite effect. Indeed, starved flies with CG-specific *AdoR* knockdown took significantly more sucrose sips than controls (Figure 4B), visited the sucrose source more often, and showed increased feeding-burst frequency (Figures S5A–S5F). This was confirmed with an independent AdoR-RNAi line (Figure S5G). Even without food deprivation, CG-deficient flies fed more than controls (Figure S5H), not only on sucrose but also on standard fly food (Figure 4C).

Using the capillary feeder (CAFE) assay, we found that flies deficient in *AdoR* in CG continued to overeat after 16 h (Figure 4D), suggesting a failure to reach satiation. We then wondered about their ability to store superfluous energy in the form of fat by measuring triacylglyceride (TAG) levels after a high-fat, high-sugar diet, which normally increases fat storage (Figure 4E). Despite consuming similar amounts as controls (Figure S5I), CG AdoR-deficient flies showed decreased TAG/protein ratios, suggesting impaired fat storage. This mirrors phenotypes seen in *AdgfA* mutants with elevated hemolymph adenosine levels,[40] implicating AdoR signaling in CG—alongside the fat body[40]—in regulating energy storage and associated behaviors.

In addition to feeding, 24-h-starved flies deficient in *AdoR* in CG did not show any difference in their running speed over multiple trials during vinegar stimulation in odor-tracking experiments (Figures 4F and 4G), while flies fed *ad libitum* ran significantly faster toward vinegar odor than controls in successive trials (Figures 4H and 4I). These flies did not show any difference in basal locomotion on the treadmill nor in their innate preference to vinegar odor (Figures S5J–S5M). However, they were more sensitive to starvation and died earlier compared to controls, consistent with an impairment in nutrient storage (Figure S5N). Taken together, these data show that appropriate energy-dependent expression of foraging and feeding behavior requires expression of *AdoR* in CG.

Together, our data show that adenosine signaling in glia modulates hunger-state-dependent behaviors, i.e., persistent foraging and feeding, differentially through at least three different types of glial cells—PNG, ALG, and CG. While AdoR in PNG promotes feeding but not foraging, AdoR signaling in ALG promotes foraging but not feeding upon starvation. By contrast, AdoR signaling in CG is required to suppress foraging and feeding in flies fed *ad libitum*.

Starvation and adenosine signaling modulate glial intracellular calcium levels

Our data highlight a critical role for adenosine signaling in glial subtypes regulating feeding and foraging behavior. We next explored how adenosine signaling in glia produces these effects. Across species, glial calcium activity often responds to neuronal activity and modulates neuronal excitability, synaptic transmission, and behavior.[7,8] In flies, glial calcium dynamics have also been linked to neuronal activity and behavior.[16,17,20,23,55–57] We therefore investigated whether starvation modulates calcium levels by using the calcium-modulated photoactivatable ratiometric integrator (CaMPARI2) as a proxy for calcium activity in explant brains (Figure 5A).[58,59]

In PNG, CaMPARI2 photoconversion did not differ between fed and 24-h-starved flies in standard saline containing D-glucose and trehalose, the main types of sugar found in the fly's hemolymph (Figures S6A and S6B). However, since hemolymph sugar levels drop during starvation,[60] we repeated the experiment in sugar-free saline.[61] Under these conditions, 24-h-starved flies showed significantly increased CaMPARI2 signal in PNG, suggesting that PNG react to low levels of sugar, or starvation, with an increase of cellular calcium (Figures 5B and 5C). Given that AdoR is required in PNG for feeding during starvation, we knocked down *AdoR* in PNG and found that it impaired the starvation-induced calcium increase, indicating that adenosine signaling is required for this effect (Figures 5B and 5C).

We then artificially elevated calcium in PNG by expressing the red-shifted channelrhodopsin CsChrimson.[62] Although glial cells are not electrically excitable, channelrhodopsins are known to be permeable to calcium cations and have been successfully used in glia to induce calcium transients.[63,64] Closed-loop optogenetic activation during feeding on the FlyPAD, triggered by proboscis contact with the sucrose drop,[65] progressively increased sucrose intake in fed flies (Figure 5E). This was accompanied by longer sip durations as well as increased activity bouts and feeding-burst frequency (Figures S5D–S5I), suggesting that our optogenetic stimulation paradigm indeed mimicked food deprivation in fed flies.

We next assessed calcium levels in CG. Starved flies again showed elevated CaMPARI2 photoconversion in CG compared to fed controls (Figures 5F and 5G). Unlike in PNG, *AdoR* knockdown in CG increased calcium in fed, but not in starved, flies, suggesting that AdoR suppresses calcium levels increase in CG under nutrient-rich conditions (Figures 5F and 5G). Remarkably, although CG also transport glucose,[26,57] the presence of D-glucose and trehalose in the saline solution did not influence calcium levels in CG in fed or starved brain, respectively (Figure S6J).

Albeit less strongly than PNG stimulation, optogenetic CG stimulation via CsChrimson also enhanced feeding behavior in

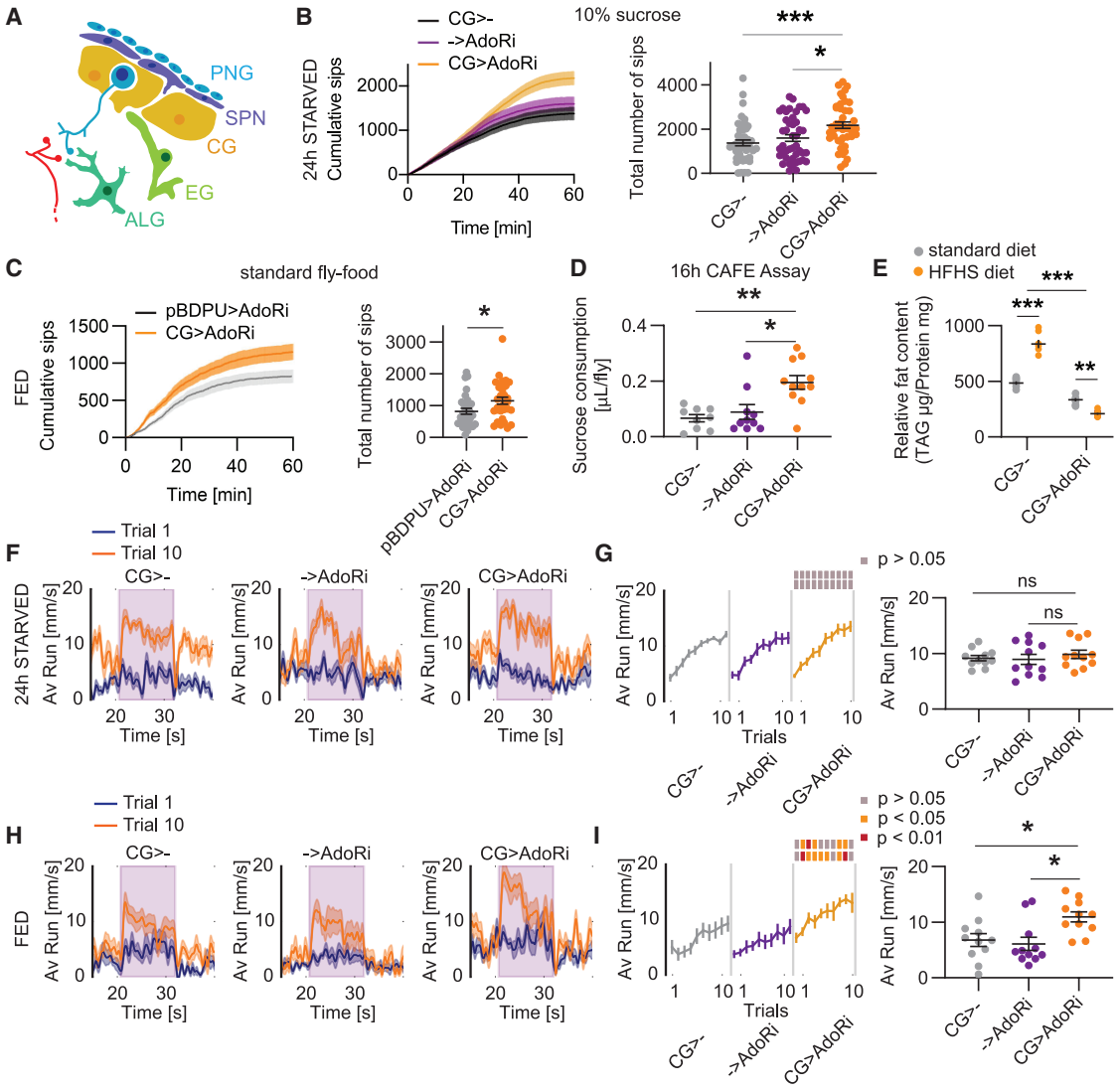

Figure 4. Adenosine signaling in cortex glia inhibits feeding and food-odor tracking behavior

(A) Anatomical location of the different glia subpopulations in the fly CNS. PNG, perineurial glia; SPN, subperineurial glia; CG, cortex glia; ALG, astrocyte-like glia; ENG, ensheathing glia.

(B) Cumulative number of sips (mean ± SEM) and total number of sips on 10% sucrose drops in 24-h-starved control flies (CG>– and –>AdoRi) or upon knockdown of AdoR in CG (CG>AdoRi; n = 45/44/44; Kruskal-Wallis test, p = 0.0006).

(C) Cumulative number of sips (mean ± SEM) and total number of sips on standard fly food drops in fed control flies (pBDPU>AdoRi) or upon knockdown of AdoR in CG (CG>AdoRi; n = 31/31; Mann-Whitney U test, p = 0.0251).

(D) Sucrose consumption of control flies (CG>– and –>AdoRi) or upon knockdown of AdoR in CG (CG>AdoRi) after 16 h in the CAFE (n = 10/10/11; Kruskal-Wallis test, p = 0.0035).

(E) Relative triacylglyceride (TAG) content in control flies (CG>–) and flies deficient for AdoR in CG (CG>AdoRi) fed on standard fly food or on high-fat-, high-sugar-containing food (HFHS; n = 8/7/8/8 replicates; 5 flies/replicate; 2-way ANOVA, p(groups) < 0.0001; p(diet) < 0.0001; p(interaction) < 0.0001).

(F) Averaged forward running speed (±SEM) in 24-h-starved control flies (CG>– and –>AdoRi) or upon knockdown of AdoR in CG (CG>AdoRi).

(G) Running speed during odor exposure (mean ± SEM; n = 11/11/11; 2-way RM ANOVA, p(groups) = 0.67; p(trials) < 0.0001; p(interaction) = 0.40). The scatterplot displays the averaged running speed over the ten trials (one-way ANOVA, p = 0.67).

(H) Averaged forward running speed (±SEM) in fed control flies (CG>– and –>AdoRi) or upon knockdown of AdoR in CG (CG>AdoRi).

(I) Running speed during odor exposure (mean ± SEM; n = 11/11/11; 2-way RM ANOVA, p(groups) = 0.0077; p(trials) < 0.0001; p(interaction) = 0.50). The scatterplot displays the averaged running speed over the ten trials (one-way ANOVA, p = 0.0077).

For food-odor tracking behavior experiments, Sidak's post hoc trial-to-trial comparisons are depicted on the top of the graphs as color-coded boxes (gray, $p > 0.05$; orange, $p < 0.05$; red, $p < 0.01$). Scatterplots display individual data points as well as the mean ± SEM for each group. Post hoc pairwise comparisons: ns, non-significant; *$p < 0.05$; **$p < 0.01$; ***$p < 0.001$. See also Figure S5.

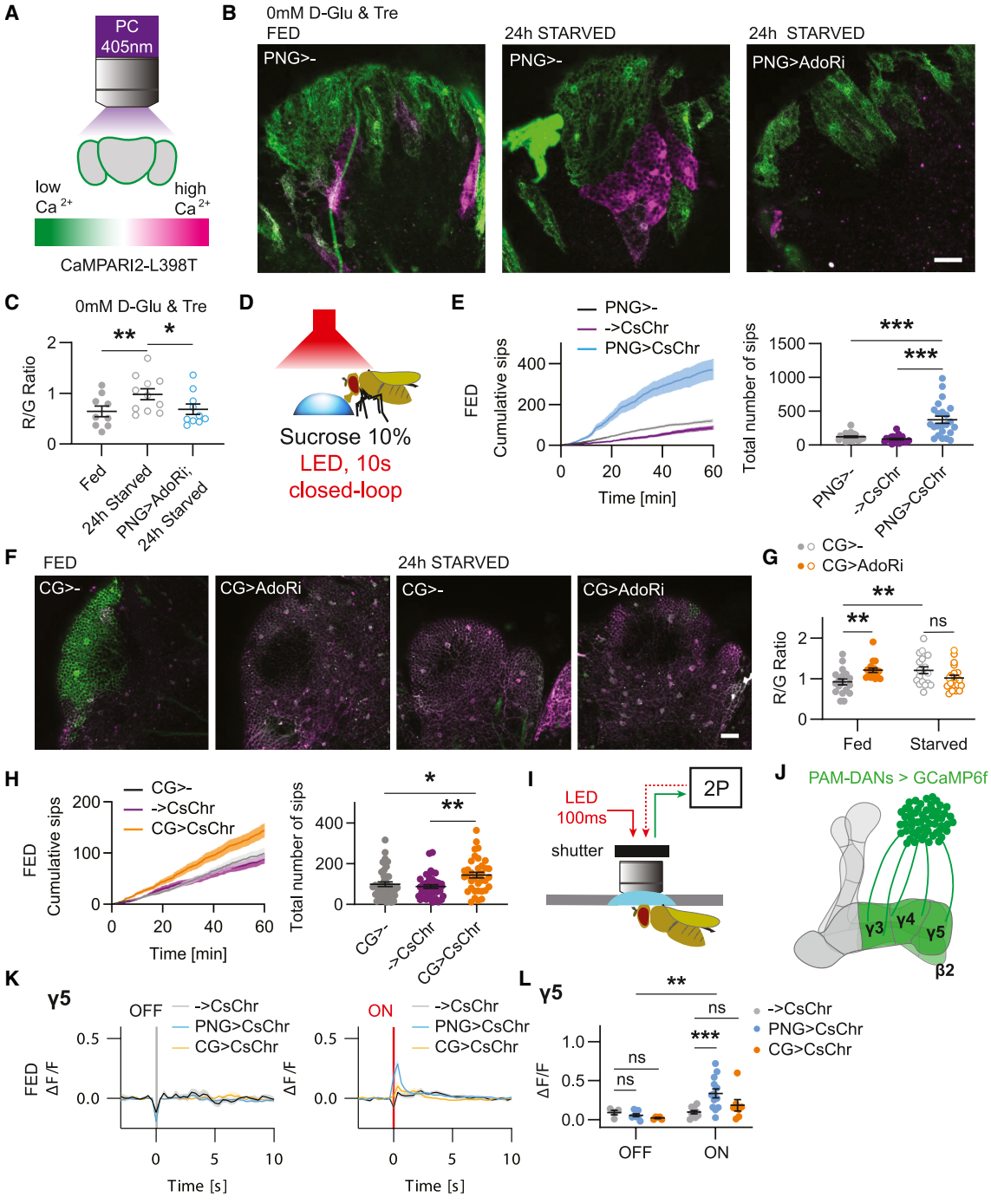

Figure 5. Starvation and adenosine signaling modulate intracellular calcium levels in perineurial and cortex glia

(A) *Ex vivo* CaMPARI imaging assessing cytoplasmic calcium accumulation. The CaMPARI protein converts from green to red fluorescence (here in magenta) in the presence of high [Ca^{2+}] and photoconversion by UV light.

(B) Example images of CaMPARI2-L398T-expressing PNG cells in dorso-caudal brain explants from fed and 24-h-starved control flies (PNG>–) and upon knockdown of AdoR (PNG>AdoRi), in sugar-free artificial hemolymph saline (AHL), after photoconversion (D-Glu, D-glucose; Tre, trehalose). Scale bar, 20 μm.

(C) Photoconversion ratios in fed and 24-h-starved control flies (n = 9/11), as well as for 24-h-starved PNG>AdoRi flies (N = 10; two-way ANOVA, p(AHL) = 0.0076; p(groups) = 0.06; p(interaction) = 0.06).

(D) Closed-loop optogenetic stimulation paradigm in the FlyPAD feeding assay. The red LED is triggered by the interaction between the fly's proboscis and the sucrose drop.

(E) Cumulative sips (mean ± SEM) and total number of sips on 10% sucrose drop in fed control flies (PNG>– and –>CsChr) or in fed flies expressing CsChrimson in PNG (PNG>CsChr; n = 23/22/23; Kruskal-Wallis test, $p < 0.0001$).

(legend continued on next page)

fed flies, increasing sip counts, activity bouts, and feeding bursts (Figures 5H, S6C, and S6K–S6P). These findings reveal a more nuanced relationship among sugar levels, glial calcium, and feeding behavior. Still, the imaging data align with our behavioral results (see Figure 4), confirming that AdoR in CG suppresses both calcium levels and feeding under fed conditions.

Since PNG and CG stimulation were sufficient to promote feeding, we hypothesized that they influence neuronal circuits. Given dopamine's role in state-dependent behaviors and prior evidence in rodents and flies demonstrating that astrocytes modulate DAN activity,[19,66–68] we focused on these modulatory neurons. Specifically, fly's DANs from the protocerebral anterior medial (PAM) cluster, which innervate the horizontal lobe of the mushroom body (MB), convey various appetitive signals, including vinegar odor and sucrose.[69–73] Using *in vivo* 2-photon imaging, we recorded PAM-DAN calcium activity while optogenetically stimulating PNG or CG (Figures 5I and 5J). A single 100-ms stimulation of PNG evoked strong calcium transients in DAN axons innervating the γ5, β2, and β′2 compartments of the MB, known to respond to sucrose taste[70,72] (Figures 5K, 5L, S7A, and S7B). In contrast, no response was observed in the γ3 compartment, also consistent with prior findings[70,72] (Figures S7E and S7F). Contrary to PNG, stimulation of CG did not evoke DAN calcium responses (Figures 5K, 5L, and S7), although we cannot rule out effects from longer stimulation, as sustained CG activation has triggered seizure-like activity in larvae.[16] We also observed small but significant responses to the light stimulus in control flies, especially in γ3 and γ4 compartments (Figures S7C–S7F), consistent with known visual responses in the fly MB.[74,75]

Altogether, our data show that AdoR signaling is responsible for the regulation of cytoplasmic calcium levels in PNG and CG. While adenosine signaling in PNG is necessary for the calcium increase we observed in starved flies, it prevents its increase in CG of fed flies. In addition, we show that optogenetic stimulation of PNG is sufficient to promote feeding in fed flies as well as to evoke calcium transients in neurons conveying sweet taste information.

Adenosine signaling in perineurial, cortex, and astrocyte-like glia alters dopaminergic neuron calcium responses in a state-dependent manner

Since PAM-DANs may mediate glial influence on behavior and AdoR is required in glia for state-dependent behavior, we tested whether AdoR in glia could modulate PAM-DAN responses to food-related cues. Using *in vivo* 2-photon microscopy, we recorded calcium responses to vinegar odor in PAM neurons in flies with *AdoR* knockdown in PNG, CG, or ALG (Figures 6A–6C).

In control flies, we observed an increased vinegar odor response in 24-h-starved flies as compared to fed flies, consistent with our previous findings[70] (Figures 6D–6G and S8). Importantly, AdoR expression in glia was required for this state-dependent modulation. Knockdown of *AdoR* in PNG increased vinegar-odor responses in the γ5 compartment of the MB in fed flies (Figures 6D and 6G, left), while no such effect was observed in the γ3 compartment (Figures 6F and 6G, right) and with intermediate changes in γ4, β2, and β′2 (Figures 6E, 6G, and S8), suggesting compartment-specific modulation, consistent with our optogenetic data (Figures 5K, 5L, and S7).

Conversely, knockdown of *AdoR* in CG or ALG decreased vinegar responses in starved flies across MB compartments (Figures 6D–6G and S8). For ALG, this matches the observed deficits in vinegar-odor tracking (Figures 3G and 3H). By contrast, the imaging data obtained on flies with *AdoR* knockdown in PNG and CG surprisingly seem to conflict with their respective phenotypes on the treadmill assay (see Figures 3E, 3F, and 4F–4I), as we expected to see no difference in the DAN response to vinegar upon knockdown of *AdoR* in PNG and an increase upon knockdown of *AdoR* in CG. This indicates that PAM-DANs may not be the primary or the only targets of PNG and CG. This is not surprising, as these neurons comprise only a part of the complex neural circuits underlying feeding and olfactory-driven behaviors, while glia is ubiquitous in the CNS. Therefore, while our data suggest that the effects of adenosine signaling in ALG might modulate foraging behavior through MB DANs, the situation appears more complex for PNG and CG.

Adenosine signals in cortex and astrocyte-like glia occur through distinct intracellular pathways

The data presented so far indicate that adenosine signals might be different in distinct glia subpopulations and in turn regulate different aspects of behavior. To gain a better understanding of the mechanisms linking adenosine signaling to glia physiology, we sought to investigate the signaling pathways downstream of AdoR activation in glia. In *Drosophila*, AdoR has been shown to activate cyclic AMP production and intracellular calcium release, suggesting coupling to Gαs- and Gαq-protein-mediated pathways (Figure 7A).[43,51]

(F) Example images of CaMPARI2-L398T-expressing CG cells in dorso-caudal brain explants from fed and 24-h-starved control flies (CG>−) and upon knockdown of AdoR (CG>AdoRi), after photoconversion. Scale bar, 20 μm.
(G) Photoconversion ratios in fed and 24-h-starved control flies (CG>−; n = 18/17) and upon knockdown of AdoR (CG>AdoRi; n = 18/20; two-way ANOVA, p(feeding state) = 0.50; p(genotype) = 0.49; p(interaction) = 0.0014; see Figure S6J).
(H) Cumulative sips (mean ± SEM) and total number of sips on 10% sucrose drops in fed control flies (CG>− and −>CsChr) or in fed flies expressing CsChrimson in CG (CG>CsChr; n = 44/41/37; Kruskal-Wallis test, p = 0.0040).
(I) Optogenetic stimulation of PNG and CG, respectively, during *in vivo* 2-photon calcium imaging in dopaminergic neurons (DANs).
(J) GCaMP6f expression pattern in the PAM-DAN cluster in the different compartments of the MB.
(K) Average (±SEM) ΔF/F calcium responses in PAM-DANs innervating the γ5 compartment of the MB to optogenetic stimulation of PNG (PNG>CsChr) and CG (CG>CsChr), respectively (gray line, LED OFF; red line, LED ON).
(L) Peak responses following the light stimulus (LED OFF: n = 4/8/5; LED ON: n = 10/13/7; two-way ANOVA, p(genotype) = 0.0837; p(LED) = 0.0015; p(interaction) = 0.0368).
Scatterplots display individual data points, as well as the mean ± SEM for each group. Post hoc pairwise comparisons: ns, non-significant; *p < 0.05; **p < 0.01; ***p < 0.001. See also Figures S6 and S7.

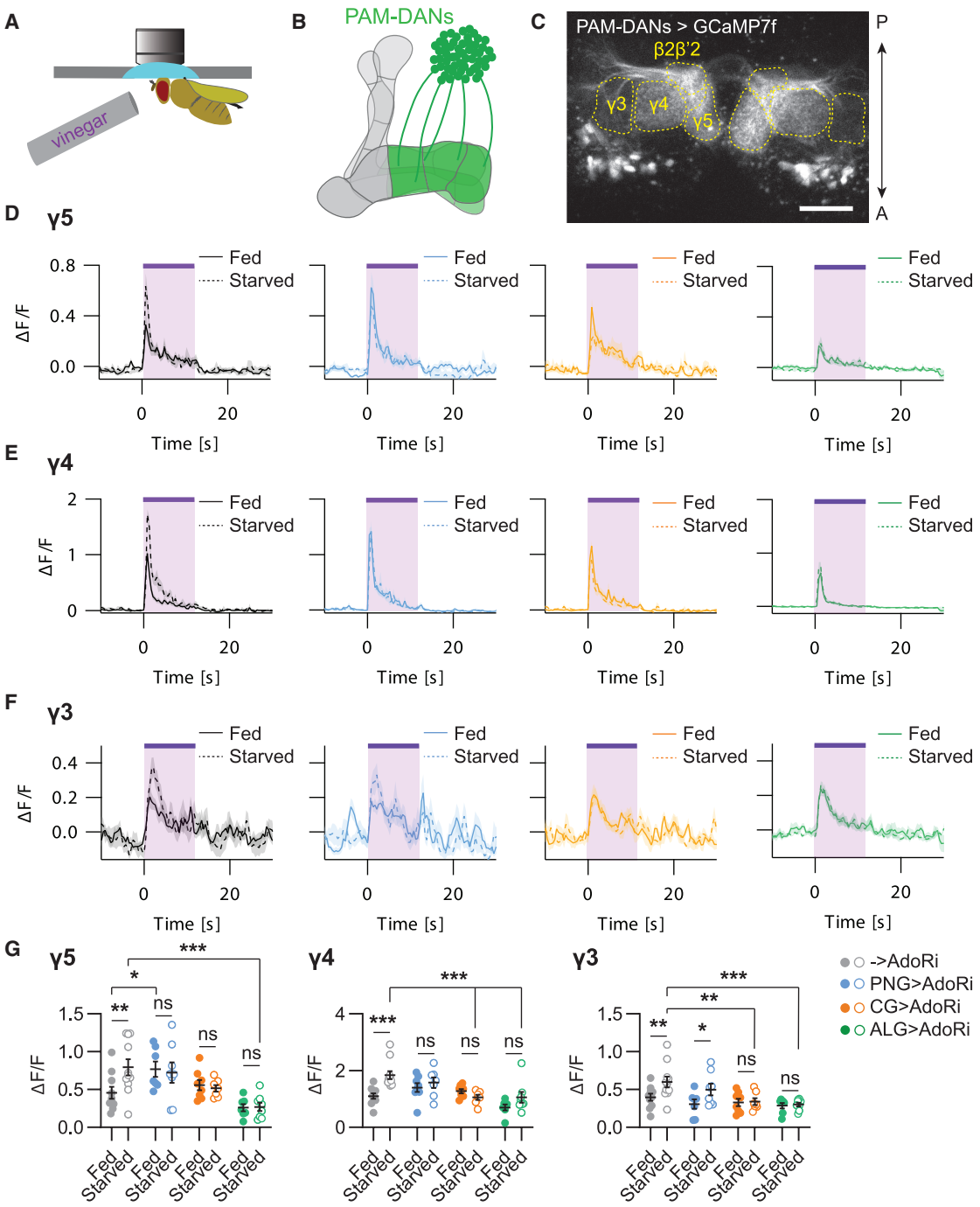

Figure 6. Adenosine signaling in perineurial, cortex, and astrocyte-like glia differentially modulates dopaminergic neuron response to vinegar in fed and starved flies

(A) Tethered flies were imaged under a 2-photon microscope and exposed to vinegar odor for 12 s.

(B) PAM-DANs innervating the horizontal lobe of the MB.

(C) Representative *z*-averaged projection image showing the PAM-DANs axons expressing GCaMP7f in the different MB compartments (GMR58E02-LexA>LexAop-GCaMP7f; A, anterior; P, posterior). Scale bar, 20 μm.

(D) Averaged ΔF/F calcium responses to vinegar-odor stimulation (purple) in the γ5 compartment in fed and 24-h-starved control flies (−>AdoRi) or in flies expressing *AdoR*-RNAi in PNG (blue; PNG>AdoRi), CG (orange; CG>AdoRi), and ALG (green; ALG>AdoRi), respectively.

(E) Averaged ΔF/F responses in the γ4 compartment.

(F) Averaged ΔF/F responses in the γ3 compartment.

(legend continued on next page)

To identify the signaling pathways downstream of AdoR activation, we knocked down *rutabaga* (adenylyl cyclase 1) and *NorpA* (phospholipase Cγ) in PNG, CG, and ALG glia. In PNG, neither knockdown altered feeding in starved flies (Figures S9A and S9B), suggesting an alternative signaling mechanism.[76] In contrast, *rutabaga* knockdown in ALG significantly reduced sucrose consumption (Figure 7B) and food-odor tracking (Figures 7C and 7D), while *NorpA* knockdown had no effect (Figures 7E and 7F). To test AdoR dependence, we fed flies with the AdoR agonist 2-chloroadenosine. Unlike controls, *rutabaga* knockdown flies failed to increase odor tracking (Figures 7G and 7H), confirming *rutabaga* as essential for AdoR signaling in ALG.

Surprisingly, *rutabaga* knockdown in CG had no effect on feeding behavior (Figure S9C), but *NorpA* knockdown increased sucrose consumption (Figure 7I), mimicking *AdoR* knockdown (Figure 4B). We confirmed these results by knocking down the genes coding for the different Gα proteins. Similar to *NorpA*, flies with a knockdown for its upstream Gαq protein in CG took a larger number of sips (Figure S9D). However, the same phenotype was also observed in flies with a knockdown for Gαi but not in flies with a knockdown for Gαs (Figure S9D). Taken together, these data suggest that both Gαq/PLCγ and Gαi-mediated pathways are required in CG for appropriate feeding behavior.

To determine whether these pathways mediate AdoR signaling, we again used the AdoR agonist 2-chloroadenosine and assessed its effect on CG intracellular calcium in explant brains from flies expressing RNAi directed against *NorpA* and *Gαi* transcripts in CG, respectively. In starved controls, 2-chloroadenosine reduced calcium in CG (Figure 7J), confirming AdoR's inhibitory effect (Figure 5F). This reduction was blocked in *NorpA*-knockdown brains, demonstrating that Gαq/PLCγ is required for AdoR function in CG. Surprisingly, Gαi knockdown caused an increase in CaMPARI2 photoconversion after AdoR agonist exposure (Figure S9F), suggesting that Gαi may not directly mediate AdoR signaling but interacts in parallel with the Gαq pathway.

In summary, AdoR signals through cell-type-specific mechanisms in glia: via Gαs/adenylyl cyclase in ALG, through Gαq/PLCγ in CG, and possibly through an unknown pathway in PNG.

DISCUSSION

Physiological states such as hunger induce a suite of adaptive behaviors, including foraging and feeding. While neuronal mechanisms underlying these behaviors have been amply documented, the role of glia remains less understood. Here, we demonstrate that adenosine signaling via its receptor, AdoR, modulates feeding-related behaviors through distinct glial subtypes in *Drosophila*. Crucially, different glial subpopulations interpret adenosine signals in subtype-specific ways. AdoR activation in PNG and ALG enhances feeding and foraging, respectively. Conversely, AdoR signaling in CG suppresses these behaviors (Figure S10).

PNG and CG have both been shown to be crucial for the transfer of nutrients to fuel the nervous system,[27,57,77–80] a role conserved in the vertebrate BBB and neurovascular unit.[24,27] Due to its anatomical location as the interface between the nutrient-containing hemolymph and the nutrient-consuming CNS, the HBB and glia in general have been proposed to function as a nutritional sensor capable of adapting the CNS to food shortages.[28,30,31,81] In addition, calcium transients have been reported in the fly PNG and CG and seem to be important in contributing to the maintenance of neuronal excitability, suggesting that they could therefore influence behavior.[16,17,56] Our results provide support for this claim, as we show here that these intracellular calcium levels are modulated by the animal's feeding state. However, in PNG, this modulation depends on the presence of sugar in the extracellular saline solution, suggesting that circulating sugar maintains low calcium activity in the PNG of fed flies, while it is not the case for CG, even though CG express glucose transporters.[26,57] This rather suggests that CG do not directly sense changes in hemolymph sugar concentration and must therefore detect the metabolic state of the fly by other mechanisms, for example via insulin signaling[57] or by detecting intracellular energetic state.[78] Interestingly, we also show in the present study that adenosine signaling is required in CG for the weight gain induced by high-fat, high-sugar diet. Although the physiological mechanisms linking glia activity to energy storage remain to be elucidated, our data highlight the role of CNS glia in the regulation of systemic energetic metabolism, a function reminiscent of the role played by astrocytes in the mouse hypothalamus.[29]

As our data primarily show a role for circulating adenosine in regulating feeding-state-dependent behavior, this implies that adenosine crosses the HBB to reach CG and ALG. Although we do not have direct evidence, it is plausible that adenosine crosses the HBB through one or more of the multiple types of transporters expressed by PNG and SPN.[50,82] Our 2-chloroadenosine bath application experiments on intact brains also suggest that adenosine can cross the HBB and reach CG. Furthermore, ATP bath application has been shown to promote or inhibit calcium activity in ALG.[21] However, we cannot exclude the participation of an independent, local production of extracellular adenosine in the fly brain. Indeed, we also observed consequences of the knockdown of *AdoR* in glia intracellular calcium levels and in their effect on neuronal activity in fed flies whose hemolymphs contain adenosine concentrations below the reported AdoR detection threshold.[40,43,51] This suggests a local amplification of the signal and/or direct production/release of adenosine by neurons or glia. Interestingly, recent work from Themparambil and colleagues showed that active neurons release ATP that, after conversion into adenosine, signals to astrocytes to promote

(G) Maximal peak responses to vinegar odor in the different groups ($n_{->AdoRi}$ = 10/11; $n_{PNG>AdoRi}$ = 8/7; $n_{CG>AdoRi}$ = 8/7; $n_{ALG>AdoRi}$ = 7/8; γ5: two-way ANOVA, p(genotype) < 0.0001, p(state) = 0.32, p(interaction) = 0.08; γ4: two-way ANOVA, p(genotype) < 0.0001, p(state) = 0.0090, p(interaction) = 0.0061; γ3: two-way ANOVA, p(genotype = 0.0021, p(state) = 0.0121, p(interaction) = 0.17).

Scatterplots display individual data points as well as mean ± SEM for each group. Post hoc pairwise comparisons: ns, non-significant; *p < 0.05; **p < 0.01; ***p < 0.001. See also Figure S8.

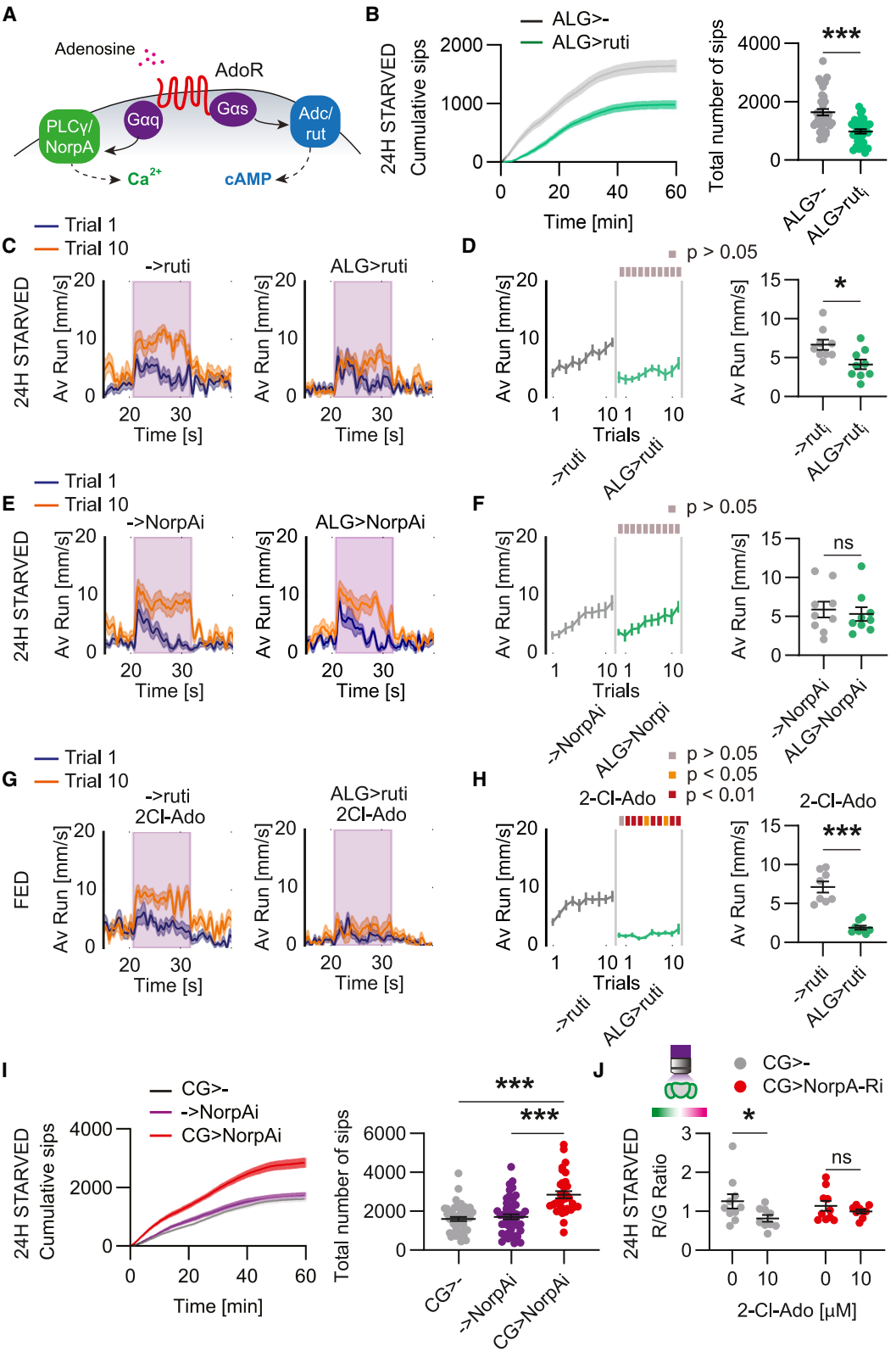

(legend on next page)

metabolic support to neuronal activity.[83] This further highlights the role of adenosine signaling in the function of the neurovascular unit that fuels neurons in response to their energy demand.[84] In the fly brain, the regulation of extracellular adenosine levels through the equilibrative nucleoside transporter-2 expressed in the MB has been shown to contribute to associative learning.[85] In addition, ATP/adenosine release by ALG modulates DAN activity and chemotaxis in fly larvae.[19] We can therefore speculate that a local, activity-dependent release of ATP/adenosine may occur in the fly brain and signal through AdoR independently of systemic, circulating adenosine. Although conceivable, the contribution of such mechanisms to behavior remains to be demonstrated by further work.

Aside from its systemic role, adenosine has been reported to act as a neuro- and gliotransmitter in various model organisms.[32,86–90] For example, adenosine signaling in striatal neurons and its interaction with dopamine modulate goal-directed behavior in mice.[91] ATP released by astrocytes and converted into adenosine inhibits feeding by modulating synaptic transmission in the hypothalamus.[10] Such mechanisms could therefore potentially be widely present in the CNS and evolutionarily well conserved.

General remarks and conclusion

With their ubiquitous presence in the CNS, glial cells are in a good position to modulate neuronal activity on a large scale and have been shown to influence neuronal activity at the level of entire networks.[7] The ways glial cells can affect neurotransmission and, in turn, behavior, are diverse and numerous. In mammals, a large variety of mechanisms used by astrocytes to modulate neuronal excitability and synaptic transmission have been described.[8] Interestingly, most of them found their equivalent in the fly's glia, in ALG, or in other cell types. Converse to what has been previously observed for the CG[16] and the PNG,[56] we report a decrease in neuronal excitability in DANs correlated with an increase in calcium levels in those cell types. Several hypotheses potentially explain this difference: (1) calcium activity in CG might be heterogeneous throughout the CNS, as already shown for PNG[56]; (2) the effect of glia activity on neurons might be different in various regions of the CNS; and (3) the decreased excitability we observed in DANs might be indirect and a result of an alteration of activity in other parts of the neural circuit. A decrease in odor response has been shown following ALG activation in the antennal lobe.[92] This suggests that glia-mediated neuromodulation is more heterogeneous than previously shown in other fly studies and in line with current knowledge of astrocyte functions in mammals and other organisms.[7,8] Although we did not address these mechanisms in the present study, we showed that the alteration of cellular physiology in three distinct subtypes of glial cells due to impaired adenosine signaling strongly affects the response of DANs to an appetitive odor.

In conclusion, in the present study we identify adenosine signaling in glia as a key modulator that helps an animal adapt its behavior according to its internal metabolic state. Our findings support the model that purinergic signaling can provide information to the brain about decreasing internal nutrient availability in order to prioritize behaviors that will restore the energy balance of the organism.[32] In addition, we show that this signaling occurs in fly glia and is differentially distributed in a glia-subtype-specific manner. This result underscores the importance of diversity and specialization of fly glia subpopulations in the modulation of behavior, which altogether recapitulates glial functions found in mammals.[8] Together, we suggest that purinergic signaling in glia and the mammalian BBB represents a functionally conserved mechanism that is used by animals to sense their internal energetic state and adjust their behavior accordingly.

Limitations of the study

Throughout this study, we used a candidate-based approach to uncover the role of adenosine signaling in feeding-state-dependent behavior, particularly in glia. However, given the

Figure 7. Adenosine signals hunger state through distinct pathways in astrocyte-like and cortex glia

(A) Intracellular signaling pathways triggered by AdoR activation. As a GPCR, AdoR can promote cyclic AMP production via Gαs protein and activation of the adenylyl cyclase (Adc or *rutabaga* [ruti] in flies). Through Gαq, AdoR can also promote the release of Ca^{2+} in the cytoplasm via IP3 production by the phospholipase Cγ (PLCγ or NorpA in flies).

(B) Cumulative number of sips (mean ± SEM) and total number of sips on 10% sucrose drops in 24-h-starved control flies (ALG>−) or upon knockdown of *rutabaga* in ALG (ALG>ruti; n = 38/31; Mann-Whitney U test, $p < 0.0001$).

(C) Averaged forward running speed (±SEM) in 24-h-starved control flies (−>ruti) or upon knockdown of *rutabaga* in ALG (ALG>ruti).

(D) Running speed during odor exposure (mean ± SEM; n = 9/9; 2-way RM ANOVA, p(groups) = 0.0124; p(trials) = 0.0023; p(interaction) = 0.38). The scatterplot displays the averaged running speed over the ten trials (unpaired t test, p = 0.0124).

(E) Averaged forward running speed (±SEM) in 24-h-starved control flies (−>NorpAi) or upon knockdown of *NorpA* in ALG (ALG>NorpAi).

(F) Running speed during odor exposure (mean ± SEM; n = 9/9; 2-way RM ANOVA, p(genotype) = 0.68; p(trials) < 0.0001; p(interaction) = 0.79). The scatterplot displays the averaged running speed over the ten trials (Mann-Whitney U test, p = 0.80).

(G) Averaged forward running speed (±SEM) in fed control flies (−>ruti) or upon knockdown of *rutabaga* in ALG (ALG>ruti). Flies were kept for 5 days on standard fly medium supplemented with 2-chloroadenosine (2-Cl-Ado; 1.65 mM).

(H) Running speed during odor exposure (mean ± SEM; n = 8/8; 2-way RM ANOVA, p(genotype) < 0.0001; p(trials) = 0.0092; p(interaction) = 0.0076). The scatterplot displays the averaged running speed over the ten trials (Welch's t test $p < 0.0001$).

(I) Cumulative number of sips (mean ± SEM) and total number of sips on 10% sucrose drops in 24-h-starved control flies (CG>− and −>NorpAi) or upon knockdown of *NorpA* in CG (CG>NorpAi; n = 47/48/22; Kruskal-Wallis test, $p < 0.0001$).

(J) CaMPARI2-L398T photoconversion ratios measured in explant brains from 24-h-starved control flies (CG>−) or upon knockdown of *NorpA* in CG (CG>NorpAi) after 10 min of 2-Cl-Ado exposure (10 M; CG>− n = 10/9; Mann-Whitney U test, p(2-Cl-Ado) = 0.0435; CG>NorpAi n = 10/9; Welch's t test, p(2-Cl-Ado) = 0.32; CG>− vs. CG>NorpAi, Mann-Whitney U test, p = 0.74).

Scatterplots display individual data points, as well as mean ± SEM for each group. Post hoc pairwise comparisons: ns, non-significant; *$p < 0.05$; **$p < 0.01$; ***$p < 0.001$. See also Figure S9.

number of potential players, this approach is not exhaustive. Indeed, purinergic signaling depends on the complex interplay among receptors, transporters, and multiple intra- and extracellular enzymes.[93] For this reason, it is difficult to pinpoint the exact endogenous source of adenosine as well as the precise contribution of systemic vs. local adenosine. The multiple roles of adenosine in glia and in neurons also raised the question of their independent or reciprocal modulation. How does the organism prevent spillover and off-target effects? We hypothesize that this regulation might occur through spatiotemporal modulation of the presence of the different actors of adenosine signaling at the cell membranes and their vicinity.

Similarly, we used DANs as neuronal candidates to assess the effect of adenosine signaling in glia on neuronal activity. Although these neurons are known to be key players in the modulation of feeding-state-dependent behaviors including the foraging assay used here, they are part of larger networks that underlie such behaviors. Given the ubiquitous distribution of glia in the CNS, many other neural circuits are most likely to be regulated by glia and purinergic signaling, as studies in other models suggest. We believe that further work using whole-brain imaging combined with glia manipulation could provide additional insights into our understanding of glia function in the regulation of neural networks.[73,94]

RESOURCE AVAILABILITY

Lead contact

Further information and requests for resources and reagents should be directed to and will be fulfilled by the lead contact, Ilona C. Grunwald Kadow (ilona.grunwald@uni-bonn.de).

Materials availability

This study did not generate new unique reagents.

Data and code availability

- Data reported in this paper will be shared by the lead contact upon request.
- This study did not report original code.
- Any additional information required to reanalyze the data reported in this study is available from the lead contact upon request.

ACKNOWLEDGMENTS

We thank Heidi Miller-Mommerskamp and Natalie Lindenberg for help in general fly husbandry. We also thank Julia von Poblotzki for help with behavior experiments. We are grateful to Karen Y. Cheng, Annika Cichy, and Aurélie Muria for their thoughtful comments on the manuscript. We thank the German Research Foundation for funding this project (GR4310/11-1, FOR2705, and TP3 to I.C.G.K.) and for funding essential research equipment (INST 217/1135-1 to I.C.G.K.). Moreover, this work was supported through the generous funding of the state of North Rhine-Westphalia to the iBehave network (to I.C.G.K.). We would like to thank the Microscopy Core Facility of the Medical Faculty at the University of Bonn for providing support and instrumentation funded by the German Research Foundation (DFG project number 169331223). C.G.-C. is funded by the German Research Foundation (DFG) under Germany's Excellence Strategy within the framework of the Munich Cluster for Systems Neurology (EXC 2145 SyNergy, ID 390857198) and the Helmholtz Excellence Network. Y.X. is funded by the Munich Cluster for Systems Neurology (EXC 2145 SyNergy, ID 390857198).

AUTHOR CONTRIBUTIONS

J.-F.D.B. and I.C.G.K. conceptualized the study and designed the experiments. J.-F.D.B. carried out and analyzed the behavioral analysis with help from J.P., T.K., and Z.N.P. J.-F.D.B. carried out and analyzed calcium imaging experiments. C.C. and R.A. designed, performed, and analyzed liquid chromatography-tandem mass spectrometry. Y.X. and C.G.-C. designed, performed, and analyzed TAG. J.-F.D.B. and I.C.G.K. wrote the manuscript.

DECLARATION OF INTERESTS

The authors declare no competing interests.

STAR★METHODS

Detailed methods are provided in the online version of this paper and include the following:

- KEY RESOURCES TABLE
- EXPERIMENTAL MODEL AND STUDY PARTICIPANT DETAILS
- METHOD DETAILS
  - FlyPAD feeding assay
  - Spherical treadmill behavioral assay
  - CApillary FEeder (CAFE) assay
  - Olfactory 4-arm maze
  - Survival analysis
  - Adenosine content
  - TAG content
  - Dye feeding assay
  - *Ex vivo* calcium imaging
  - *In vivo* 2-photon calcium imaging
- QUANTIFICATION AND STATISTICAL ANALYSIS

SUPPLEMENTAL INFORMATION

Supplemental information can be found online at https://doi.org/10.1016/j.celrep.2025.115765.

Received: September 9, 2024
Revised: March 28, 2025
Accepted: May 9, 2025

REFERENCES

1. Rolls, E.T. (2006). Brain mechanisms underlying flavour and appetite. Philos. Trans. R. Soc. Lond. B Biol. Sci. *361*, 1123–1136. https://doi.org/10.1098/rstb.2006.1852.
2. Itskov, P.M., and Ribeiro, C. (2013). The Dilemmas of the Gourmet Fly: The Molecular and Neuronal Mechanisms of Feeding and Nutrient Decision Making in Drosophila. Front. Neurosci. *7*, 12. https://doi.org/10.3389/fnins.2013.00012.
3. Cichy, A. (2022). How the body rules the nose. Neuroform *28*, 151–158. https://doi.org/10.1515/nf-2022-0003.
4. Sachse, S., and Beshel, J. (2016). The good, the bad, and the hungry: how the central brain codes odor valence to facilitate food approach in Drosophila. Curr. Opin. Neurobiol. *40*, 53–58. https://doi.org/10.1016/j.conb.2016.06.012.
5. Sayin, S., Boehm, A.C., Kobler, J.M., De Backer, J.-F., and Grunwald Kadow, I.C. (2018). Internal State Dependent Odor Processing and Perception—The Role of Neuromodulation in the Fly Olfactory System. Front. Cell. Neurosci. *12*, 11. https://doi.org/10.3389/fncel.2018.00011.
6. Bazargani, N., and Attwell, D. (2016). Astrocyte calcium signaling: the third wave. Nat. Neurosci. *19*, 182–189. https://doi.org/10.1038/nn.4201.

7. Araque, A., Carmignoto, G., Haydon, P.G., Oliet, S.H.R., Robitaille, R., and Volterra, A. (2014). Gliotransmitters travel in time and space. Neuron *81*, 728–739. https://doi.org/10.1016/j.neuron.2014.02.007.

8. Nagai, J., Yu, X., Papouin, T., Cheong, E., Freeman, M.R., Monk, K.R., Hastings, M.H., Haydon, P.G., Rowitch, D., Shaham, S., and Khakh, B. S. (2021). Behaviorally consequential astrocytic regulation of neural circuits. Neuron *109*, 576–596. https://doi.org/10.1016/j.neuron.2020.12.008.

9. Chen, N., Sugihara, H., Kim, J., Fu, Z., Barak, B., Sur, M., Feng, G., and Han, W. (2016). Direct modulation of GFAP-expressing glia in the arcuate nucleus bi-directionally regulates feeding. Elife *5*, e18716. https://doi.org/10.7554/eLife.18716.

10. Yang, L., Qi, Y., and Yang, Y. (2015). Astrocytes Control Food Intake by Inhibiting AGRP Neuron Activity via Adenosine A1 Receptors. Cell Rep. *11*, 798–807. https://doi.org/10.1016/j.celrep.2015.04.002.

11. García-Cáceres, C., Balland, E., Prevot, V., Luquet, S., Woods, S.C., Koch, M., Horvath, T.L., Yi, C.-X., Chowen, J.A., Verkhratsky, A., et al. (2019). Role of astrocytes, microglia, and tanycytes in brain control of systemic metabolism. Nat. Neurosci. *22*, 7–14. https://doi.org/10.1038/s41593-018-0286-y.

12. Herrera Moro Chao, D., Kirchner, M.K., Pham, C., Foppen, E., Denis, R. G.P., Castel, J., Morel, C., Montalban, E., Hassouna, R., Bui, L.-C., et al. (2022). Hypothalamic astrocytes control systemic glucose metabolism and energy balance. Cell Metab. *34*, 1532–1547.e6. https://doi.org/10.1016/j.cmet.2022.09.002.

13. Zwarts, L., Van Eijs, F., and Callaerts, P. (2015). Glia in Drosophila behavior. J. Comp. Physiol. *201*, 879–893. https://doi.org/10.1007/s00359-014-0952-9.

14. Kremer, M.C., Jung, C., Batelli, S., Rubin, G.M., and Gaul, U. (2017). The glia of the adult *Drosophila* nervous system: Glia Anatomy in Adult Drosophila Nervous System. Glia *65*, 606–638. https://doi.org/10.1002/glia.23115.

15. Yildirim, K., Petri, J., Kottmeier, R., and Klämbt, C. (2019). Drosophila glia: Few cell types and many conserved functions: YILDIRIM et al. Glia *67*, 5–26. https://doi.org/10.1002/glia.23459.

16. Melom, J.E., and Littleton, J.T. (2013). Mutation of a NCKX Eliminates Glial Microdomain Calcium Oscillations and Enhances Seizure Susceptibility. J. Neurosci. *33*, 1169–1178. https://doi.org/10.1523/JNEUROSCI.3920-12.2013.

17. Weiss, S., Melom, J.E., Ormerod, K.G., Zhang, Y.V., and Littleton, J.T. (2019). Glial Ca2+signaling links endocytosis to K+ buffering around neuronal somas to regulate excitability. Elife *8*, e44186. https://doi.org/10.7554/eLife.44186.

18. Basu, R., Preat, T., and Plaçais, P.-Y. (2024). Glial metabolism versatility regulates mushroom body-driven behavioral output in Drosophila. Learn. Mem. Cold Spring Harb. N *31*, a053823. https://doi.org/10.1101/lm.053823.123.

19. Ma, Z., Stork, T., Bergles, D.E., and Freeman, M.R. (2016). Neuromodulators signal through astrocytes to alter neural circuit activity and behaviour. Nature *539*, 428–432. https://doi.org/10.1038/nature20145.

20. Blum, I.D., Keleş, M.F., Baz, E.-S., Han, E., Park, K., Luu, S., Issa, H., Brown, M., Ho, M.C.W., Tabuchi, M., et al. (2021). Astroglial Calcium Signaling Encodes Sleep Need in Drosophila. Curr. Biol. *31*, 150–162.e7. https://doi.org/10.1016/j.cub.2020.10.012.

21. Park, A., Croset, V., Otto, N., Agarwal, D., Treiber, C.D., Meschi, E., Sims, D., and Waddell, S. (2022). Gliotransmission of D-serine promotes thirst-directed behaviors in Drosophila. Curr. Biol. *32*, 3952–3970.e8. https://doi.org/10.1016/j.cub.2022.07.038.

22. Miyashita, T., Murakami, K., Kikuchi, E., Ofusa, K., Mikami, K., Endo, K., Miyaji, T., Moriyama, S., Konno, K., Muratani, H., et al. (2023). Glia transmit negative valence information during aversive learning in *Drosophila*. Science *382*, eadf7429. https://doi.org/10.1126/science.adf7429.

23. Flores-Valle, A., Vishniakou, I., and Seelig, J.D. (2025). Dynamics of glia and neurons regulate homeostatic rest, sleep and feeding behavior in Drosophila. Nat. Neurosci. Published online April 21, 2025. https://doi.org/10.1038/s41593-025-01942-1.

24. Schirmeier, S., and Klämbt, C. (2015). The Drosophila blood-brain barrier as interface between neurons and hemolymph. Mech. Dev. *138*, 50–55. https://doi.org/10.1016/j.mod.2015.06.002.

25. O'Brown, N.M., Pfau, S.J., and Gu, C. (2018). Bridging barriers: a comparative look at the blood–brain barrier across organisms. Genes Dev. *32*, 466–478. https://doi.org/10.1101/gad.309823.117.

26. Volkenhoff, A., Hirrlinger, J., Kappel, J.M., Klämbt, C., and Schirmeier, S. (2018). Live imaging using a FRET glucose sensor reveals glucose delivery to all cell types in the Drosophila brain. J. Insect Physiol. *106*, 55–64. https://doi.org/10.1016/j.jinsphys.2017.07.010.

27. Volkenhoff, A., Weiler, A., Letzel, M., Stehling, M., Klämbt, C., and Schirmeier, S. (2015). Glial Glycolysis Is Essential for Neuronal Survival in Drosophila. Cell Metab. *22*, 437–447. https://doi.org/10.1016/j.cmet.2015.07.006.

28. Rittschof, C.C., and Schirmeier, S. (2018). Insect models of central nervous system energy metabolism and its links to behavior. Glia *66*, 1160–1175. https://doi.org/10.1002/glia.23235.

29. Murat, C.D.B., and García-Cáceres, C. (2021). Astrocyte Gliotransmission in the Regulation of Systemic Metabolism. Metabolites *11*, 732. https://doi.org/10.3390/metabo11110732.

30. De Backer, J.-F., and Grunwald Kadow, I.C. (2022). A role for glia in cellular and systemic metabolism: insights from the fly. Curr. Opin. Insect Sci. *53*, 100947. https://doi.org/10.1016/j.cois.2022.100947.

31. Contreras, E.G., and Sierralta, J. (2022). The Fly Blood-Brain Barrier Fights Against Nutritional Stress. Neurosci. Insights *17*, 26331055221120252. https://doi.org/10.1177/26331055221120252.

32. Lezmy, J. (2023). How astrocytic ATP shapes neuronal activity and brain circuits. Curr. Opin. Neurobiol. *79*, 102685. https://doi.org/10.1016/j.conb.2023.102685.

33. Yegutkin, G.G. (2008). Nucleotide- and nucleoside-converting ectoenzymes: Important modulators of purinergic signalling cascade. Biochim. Biophys. Acta *1783*, 673–694. https://doi.org/10.1016/j.bbamcr.2008.01.024.

34. Buck, L.T. (2004). Adenosine as a signal for ion channel arrest in anoxia-tolerant organisms. Comp. Biochem. Physiol. B Biochem. Mol. Biol. *139*, 401–414. https://doi.org/10.1016/j.cbpc.2004.04.002.

35. Newby, A.C. (1984). Adenosine and the concept of 'retaliatory metabolites. Trends Biochem. Sci. *9*, 42–44. https://doi.org/10.1016/0968-0004(84)90176-2.

36. Haskó, G., Deitch, E.A., Szabó, C., Németh, Z.H., and Vizi, E.S. (2002). Adenosine: a potential mediator of immunosuppression in multiple organ failure. Curr. Opin. Pharmacol. *2*, 440–444. https://doi.org/10.1016/s1471-4892(02)00172-8.

37. Davis, J.M., Zhao, Z., Stock, H.S., Mehl, K.A., Buggy, J., and Hand, G.A. (2003). Central nervous system effects of caffeine and adenosine on fatigue. Am. J. Physiol. Regul. Integr. Comp. Physiol. *284*, R399–R404. https://doi.org/10.1152/ajpregu.00386.2002.

38. Antonioli, L., Csóka, B., Fornai, M., Colucci, R., Kókai, E., Blandizzi, C., and Haskó, G. (2014). Adenosine and inflammation: what's new on the horizon? Drug Discov. Today *19*, 1051–1068. https://doi.org/10.1016/j.drudis.2014.02.010.

39. Koupenova, M., and Ravid, K. (2013). Adenosine, Adenosine Receptors and Their Role in Glucose Homeostasis and Lipid Metabolism. J. Cell. Physiol. *228*, 1703–1712. https://doi.org/10.1002/jcp.24352.

40. Zuberova, M., Fenckova, M., Simek, P., Janeckova, L., and Dolezal, T. (2010). Increased extracellular adenosine in Drosophila that are deficient in adenosine deaminase activates a release of energy stores leading to wasting and death. Dis. Model. Mech. *3*, 773–784. https://doi.org/10.1242/dmm.005389.

41. Bajgar, A., Kucerova, K., Jonatova, L., Tomcala, A., Schneedorferova, I., Okrouhlik, J., and Dolezal, T. (2015). Extracellular adenosine mediates a systemic metabolic switch during immune response. PLoS Biol. *13*, e1002135. https://doi.org/10.1371/journal.pbio.1002135.

42. Bajgar, A., and Dolezal, T. (2018). Extracellular adenosine modulates host-pathogen interactions through regulation of systemic metabolism during immune response in Drosophila. PLoS Pathog. *14*, e1007022. https://doi.org/10.1371/journal.ppat.1007022.

43. Kucerova, L., Broz, V., Fleischmannova, J., Santruckova, E., Sidorov, R., Dolezal, V., and Zurovec, M. (2012). Characterization of the *Drosophila* adenosine receptor: the effect of adenosine analogs on cAMP signaling in *Drosophila* cells and their utility for *in vivo* experiments. J. Neurochem. *121*, 383–395. https://doi.org/10.1111/j.1471-4159.2012.07701.x.

44. Itskov, P.M., Moreira, J.-M., Vinnik, E., Lopes, G., Safarik, S., Dickinson, M.H., and Ribeiro, C. (2014). Automated monitoring and quantitative analysis of feeding behaviour in Drosophila. Nat. Commun. *5*, 4560. https://doi.org/10.1038/ncomms5560.

45. Davis, J.D., and Smith, G.P. (1992). Analysis of the microstructure of the rhythmic tongue movements of rats ingesting maltose and sucrose solutions. Behav. Neurosci. *106*, 217–228.

46. Sayin, S., De Backer, J.-F., Siju, K.P., Wosniack, M.E., Lewis, L.P., Frisch, L.-M., Gansen, B., Schlegel, P., Edmondson-Stait, A., Sharifi, N., et al. (2019). A Neural Circuit Arbitrates between Persistence and Withdrawal in Hungry Drosophila. Neuron *104*, 544–558.e6. https://doi.org/10.1016/j.neuron.2019.07.028.

47. Zurovec, M., Dolezal, T., Gazi, M., Pavlova, E., and Bryant, P.J. (2002). Adenosine deaminase-related growth factors stimulate cell proliferation in *Drosophila* by depleting extracellular adenosine. Proc. Natl. Acad. Sci. *99*, 4403–4408. https://doi.org/10.1073/pnas.062059699.

48. Dolezal, T., Dolezelova, E., Zurovec, M., and Bryant, P.J. (2005). A Role for Adenosine Deaminase in Drosophila Larval Development. PLoS Biol. *3*, e201. https://doi.org/10.1371/journal.pbio.0030201.

49. Novakova, M., and Dolezal, T. (2011). Expression of Drosophila Adenosine Deaminase in Immune Cells during Inflammatory Response. PLoS One *6*, e17741. https://doi.org/10.1371/journal.pone.0017741.

50. Davie, K., Janssens, J., Koldere, D., De Waegeneer, M., Pech, U., Kreft, Ł., Aibar, S., Makhzami, S., Christiaens, V., Bravo González-Blas, C., et al. (2018). A Single-Cell Transcriptome Atlas of the Aging Drosophila Brain. Cell *174*, 982–998.e20. https://doi.org/10.1016/j.cell.2018.05.057.

51. Dolezelova, E., Nothacker, H.-P., Civelli, O., Bryant, P.J., and Zurovec, M. (2007). A Drosophila adenosine receptor activates cAMP and calcium signaling. Insect Biochem. Mol. Biol. *37*, 318–329. https://doi.org/10.1016/j.ibmb.2006.12.003.

52. Roman, G., Endo, K., Zong, L., and Davis, R.L. (2001). P{Switch}, a system for spatial and temporal control of gene expression in *Drosophila melanogaster*. Proc. Natl. Acad. Sci. *98*, 12602–12607. https://doi.org/10.1073/pnas.221303998.

53. Bhattacharya, D., Górska-Andrzejak, J., Abaquita, T.A.L., and Pyza, E. (2023). Effects of adenosine receptor overexpression and silencing in neurons and glial cells on lifespan, fitness, and sleep of Drosophila melanogaster. Exp. Brain Res. *241*, 1887–1904. https://doi.org/10.1007/s00221-023-06649-y.

54. McGuire, S.E., Mao, Z., and Davis, R.L. (2004). Spatiotemporal Gene Expression Targeting with the TARGET and Gene-Switch Systems in *Drosophila*. Sci. STKE *2004*, pl6. https://doi.org/10.1126/stke.2202004pl6.

55. Holcroft, C.E., Jackson, W.D., Lin, W.-H., Bassiri, K., Baines, R.A., and Phelan, P. (2013). Innexins Ogre and Inx2 are required in glial cells for normal postembryonic development of the *Drosophila* central nervous system. J. Cell Sci. *126*, 3823–3834. https://doi.org/10.1242/jcs.117994.

56. Weiss, S., Clamon, L.C., Manoim, J.E., Ormerod, K.G., Parnas, M., and Littleton, J.T. (2022). Glial ER and GAP junction mediated Ca^{2+} waves are crucial to maintain normal brain excitability. Glia *70*, 123–144. https://doi.org/10.1002/glia.24092.

57. de Tredern, E., Rabah, Y., Pasquer, L., Minatchy, J., Plaçais, P.-Y., and Preat, T. (2021). Glial glucose fuels the neuronal pentose phosphate pathway for long-term memory. Cell Rep. *36*, 109620. https://doi.org/10.1016/j.celrep.2021.109620.

58. Fosque, B.F., Sun, Y., Dana, H., Yang, C.-T., Ohyama, T., Tadross, M.R., Patel, R., Zlatic, M., Kim, D.S., Ahrens, M.B., et al. (2015). Neural circuits. Labeling of active neural circuits in vivo with designed calcium integrators. Science *347*, 755–760. https://doi.org/10.1126/science.1260922.

59. Moeyaert, B., Holt, G., Madangopal, R., Perez-Alvarez, A., Fearey, B.C., Trojanowski, N.F., Ledderose, J., Zolnik, T.A., Das, A., Patel, D., et al. (2018). Improved methods for marking active neuron populations. Nat. Commun. *9*, 4440. https://doi.org/10.1038/s41467-018-06935-2.

60. Dus, M., Ai, M., and Suh, G.S.B. (2013). Taste-independent nutrient selection is mediated by a brain-specific Na+/solute co-transporter in Drosophila. Nat. Neurosci. *16*, 526–528. https://doi.org/10.1038/nn.3372.

61. Plaçais, P.-Y., and Preat, T. (2013). To Favor Survival Under Food Shortage, the Brain Disables Costly Memory. Science *339*, 440–442. https://doi.org/10.1126/science.1226018.

62. Klapoetke, N.C., Murata, Y., Kim, S.S., Pulver, S.R., Birdsey-Benson, A., Cho, Y.K., Morimoto, T.K., Chuong, A.S., Carpenter, E.J., Tian, Z., et al. (2014). Independent optical excitation of distinct neural populations. Nat. Methods *11*, 338–346. https://doi.org/10.1038/nmeth.2836.

63. Nagel, G., Szellas, T., Huhn, W., Kateriya, S., Adeishvili, N., Berthold, P., Ollig, D., Hegemann, P., and Bamberg, E. (2003). Channelrhodopsin-2, a directly light-gated cation-selective membrane channel. Proc. Natl. Acad. Sci. *100*, 13940–13945. https://doi.org/10.1073/pnas.1936192100.

64. Perea, G., Yang, A., Boyden, E.S., and Sur, M. (2014). Optogenetic astrocyte activation modulates response selectivity of visual cortex neurons in vivo. Nat. Commun. *5*, 3262. https://doi.org/10.1038/ncomms4262.

65. Moreira, J.-M., Itskov, P.M., Goldschmidt, D., Baltazar, C., Steck, K., Tastekin, I., Walker, S.J., and Ribeiro, C. (2019). optoPAD, a closed-loop optogenetics system to study the circuit basis of feeding behaviors. Elife *8*, e43924. https://doi.org/10.7554/eLife.43924.

66. Gomez, J.A., Perkins, J.M., Beaudoin, G.M., Cook, N.B., Quraishi, S.A., Szoeke, E.A., Thangamani, K., Tschumi, C.W., Wanat, M.J., Maroof, A. M., et al. (2019). Ventral tegmental area astrocytes orchestrate avoidance and approach behavior. Nat. Commun. *10*, 1455. https://doi.org/10.1038/s41467-019-09131-y.

67. Requie, L.M., Gómez-Gonzalo, M., Speggiorin, M., Managò, F., Melone, M., Congiu, M., Chiavegato, A., Lia, A., Zonta, M., Losi, G., et al. (2022). Astrocytes mediate long-lasting synaptic regulation of ventral tegmental area dopamine neurons. Nat. Neurosci. *25*, 1639–1650. https://doi.org/10.1038/s41593-022-01193-4.

68. Yang, J., Chen, J., Liu, Y., Chen, K.H., Baraban, J.M., and Qiu, Z. (2023). Ventral tegmental area astrocytes modulate cocaine reward by tonically releasing GABA. Neuron *111*, 1104–1117.e6. https://doi.org/10.1016/j.neuron.2022.12.033.

69. Aso, Y., Hattori, D., Yu, Y., Johnston, R.M., Iyer, N.A., Ngo, T.T.B., Dionne, H., Abbott, L.F., Axel, R., Tanimoto, H., and Rubin, G.M. (2014). The neuronal architecture of the mushroom body provides a logic for associative learning. Elife *3*, e04577. https://doi.org/10.7554/eLife.04577.

70. Siju, K.P., Štih, V., Aimon, S., Gjorgjieva, J., Portugues, R., and Grunwald Kadow, I.C. (2020). Valence and State-Dependent Population Coding in Dopaminergic Neurons in the Fly Mushroom Body. Curr. Biol. *30*, 2104–2115.e4. https://doi.org/10.1016/j.cub.2020.04.037.

71. May, C.E., Rosander, J., Gottfried, J., Dennis, E., and Dus, M. (2020). Dietary sugar inhibits satiation by decreasing the central processing of sweet taste. Elife *9*, e54530. https://doi.org/10.7554/eLife.54530.

72. Zolin, A., Cohn, R., Pang, R., Siliciano, A.F., Fairhall, A.L., and Ruta, V. (2021). Context-dependent representations of movement in Drosophila dopaminergic reinforcement pathways. Nat. Neurosci. *24*, 1555–1566. https://doi.org/10.1038/s41593-021-00929-y.

73. Aimon, S., Cheng, K.Y., Gjorgjieva, J., and Grunwald Kadow, I.C. (2023). Global change in brain state during spontaneous and forced walk in Drosophila is composed of combined activity patterns of different neuron classes. Elife *12*, e85202. https://doi.org/10.7554/eLife.85202.

74. Vogt, K., Schnaitmann, C., Dylla, K.V., Knapek, S., Aso, Y., Rubin, G.M., and Tanimoto, H. (2014). Shared mushroom body circuits underlie visual and olfactory memories in Drosophila. Elife *3*, e02395. https://doi.org/10.7554/eLife.02395.

75. Vogt, K., Aso, Y., Hige, T., Knapek, S., Ichinose, T., Friedrich, A.B., Turner, G.C., Rubin, G.M., and Tanimoto, H. (2016). Direct neural pathways convey distinct visual information to Drosophila mushroom bodies. Elife *5*, e14009. https://doi.org/10.7554/eLife.14009.

76. Boison, D., Chen, J.-F., and Fredholm, B.B. (2010). Adenosine signaling and function in glial cells. Cell Death Differ. *17*, 1071–1082. https://doi.org/10.1038/cdd.2009.131.

77. Delgado, M.G., Oliva, C., López, E., Ibacache, A., Galaz, A., Delgado, R., Barros, L.F., and Sierralta, J. (2018). Chaski, a novel Drosophila lactate/pyruvate transporter required in glia cells for survival under nutritional stress. Sci. Rep. *8*, 1186. https://doi.org/10.1038/s41598-018-19595-5.

78. Silva, B., Mantha, O.L., Schor, J., Pascual, A., Plaçais, P.-Y., Pavlowsky, A., and Preat, T. (2022). Glia fuel neurons with locally synthesized ketone bodies to sustain memory under starvation. Nat. Metab. *4*, 213–224. https://doi.org/10.1038/s42255-022-00528-6.

79. Rabah, Y., Francés, R., Minatchy, J., Guédon, L., Desnous, C., Plaçais, P.-Y., and Preat, T. (2023). Glycolysis-derived alanine from glia fuels neuronal mitochondria for memory in Drosophila. Nat. Metab. *5*, 2002–2019. https://doi.org/10.1038/s42255-023-00910-y.

80. Haynes, P.R., Pyfrom, E.S., Li, Y., Stein, C., Cuddapah, V.A., Jacobs, J. A., Yue, Z., and Sehgal, A. (2024). A neuron-glia lipid metabolic cycle couples daily sleep to mitochondrial homeostasis. Nat. Neurosci. *27*, 666–678. https://doi.org/10.1038/s41593-023-01568-1.

81. McMullen, E., Hertenstein, H., Strassburger, K., Deharde, L., Brankatschk, M., and Schirmeier, S. (2023). Glycolytically impaired Drosophila glial cells fuel neural metabolism via β-oxidation. Nat. Commun. *14*, 2996. https://doi.org/10.1038/s41467-023-38813-x.

82. Featherstone, D.E. (2011). Glial solute carrier transporters in *drosophila* and mice. Glia *59*, 1351–1363. https://doi.org/10.1002/glia.21085.

83. Theparambil, S.M., Kopach, O., Braga, A., Nizari, S., Hosford, P.S., Sagi-Kiss, V., Hadjihambi, A., Konstantinou, C., Esteras, N., Gutierrez Del Arroyo, A., et al. (2024). Adenosine signalling to astrocytes coordinates brain metabolism and function. Nature *632*, 139–146. https://doi.org/10.1038/s41586-024-07611-w.

84. Nortley, R., and Attwell, D. (2017). Control of brain energy supply by astrocytes. Curr. Opin. Neurobiol. *47*, 80–85. https://doi.org/10.1016/j.conb.2017.09.012.

85. Knight, D., Harvey, P.J., Iliadi, K.G., Klose, M.K., Iliadi, N., Dolezelova, E., Charlton, M.P., Zurovec, M., and Boulianne, G.L. (2010). Equilibrative Nucleoside Transporter 2 Regulates Associative Learning and Synaptic Function in *Drosophila*. J. Neurosci. *30*, 5047–5057. https://doi.org/10.1523/JNEUROSCI.6241-09.2010.

86. Halassa, M.M., Florian, C., Fellin, T., Munoz, J.R., Lee, S.-Y., Abel, T., Haydon, P.G., and Frank, M.G. (2009). Astrocytic Modulation of Sleep Homeostasis and Cognitive Consequences of Sleep Loss. Neuron *61*, 213–219. https://doi.org/10.1016/j.neuron.2008.11.024.

87. Martin-Fernandez, M., Jamison, S., Robin, L.M., Zhao, Z., Martin, E.D., Aguilar, J., Benneyworth, M.A., Marsicano, G., and Araque, A. (2017). Synapse-specific astrocyte gating of amygdala-related behavior. Nat. Neurosci. *20*, 1540–1548. https://doi.org/10.1038/nn.4649.

88. Illes, P., Burnstock, G., and Tang, Y. (2019). Astroglia-Derived ATP Modulates CNS Neuronal Circuits. Trends Neurosci. *42*, 885–898. https://doi.org/10.1016/j.tins.2019.09.006.

89. Corkrum, M., Covelo, A., Lines, J., Bellocchio, L., Pisansky, M., Loke, K., Quintana, R., Rothwell, P.E., Lujan, R., Marsicano, G., et al. (2020). Dopamine-Evoked Synaptic Regulation in the Nucleus Accumbens Requires Astrocyte Activity. Neuron *105*, 1036–1047.e5. https://doi.org/10.1016/j.neuron.2019.12.026.

90. Chen, A.B., Duque, M., Wang, V.M., Dhanasekar, M., Mi, X., Rymbek, A., Tocquer, L., Narayan, S., Prober, D., Yu, G., et al. (2024). Norepinephrine changes behavioral state via astroglial purinergic signaling. Preprint at bioRxiv. https://doi.org/10.1101/2024.05.23.595576.

91. Chen, J.-F., Choi, D.-S., and Cunha, R.A. (2023). Striatopallidal adenosine A2A receptor modulation of goal-directed behavior: Homeostatic control with cognitive flexibility. Neuropharmacology *226*, 109421. https://doi.org/10.1016/j.neuropharm.2023.109421.

92. Liu, H., Zhou, B., Yan, W., Lei, Z., Zhao, X., Zhang, K., and Guo, A. (2014). Astrocyte-like glial cells physiologically regulate olfactory processing through the modification of ORN - PN synaptic strength in *D rosophila*. Eur. J. Neurosci. *40*, 2744–2754. https://doi.org/10.1111/ejn.12646.

93. Volonté, C., Alberti, F., Vitale, G., and Liguori, F. (2022). Delineating Purinergic Signaling in Drosophila. Int. J. Mol. Sci. *23*, 15196. https://doi.org/10.3390/ijms232315196.

94. Aimon, S., Katsuki, T., Jia, T., Grosenick, L., Broxton, M., Deisseroth, K., Sejnowski, T.J., and Greenspan, R.J. (2019). Fast near-whole-brain imaging in adult Drosophila during responses to stimuli and behavior. PLoS Biol. *17*, e2006732. https://doi.org/10.1371/journal.pbio.2006732.

95. Pologruto, T.A., Sabatini, B.L., and Svoboda, K. (2003). ScanImage: flexible software for operating laser scanning microscopes. Biomed. Eng. Online *2*, 13. https://doi.org/10.1186/1475-925X-2-13.

96. Ja, W.W., Carvalho, G.B., Mak, E.M., De La Rosa, N.N., Fang, A.Y., Liong, J.C., Brummel, T., and Benzer, S. (2007). Prandiology of *Drosophila* and the CAFE assay. Proc. Natl. Acad. Sci. *104*, 8253–8256. https://doi.org/10.1073/pnas.0702726104.

97. Kobler, J.M., Rodriguez Jimenez, F.J., Petcu, I., and Grunwald Kadow, I. C. (2020). Immune Receptor Signaling and the Mushroom Body Mediate Post-ingestion Pathogen Avoidance. Curr. Biol. *30*, 4693–4709.e3. https://doi.org/10.1016/j.cub.2020.09.022.

98. Lewis, L.P.C., Siju, K.P., Aso, Y., Friedrich, A.B., Bulteel, A.J.B., Rubin, G. M., and Grunwald Kadow, I.C. (2015). A Higher Brain Circuit for Immediate Integration of Conflicting Sensory Information in Drosophila. Curr. Biol. *25*, 2203–2214. https://doi.org/10.1016/j.cub.2015.07.015.

99. Coman, C., Solari, F.A., Hentschel, A., Sickmann, A., Zahedi, R.P., and Ahrends, R. (2016). Simultaneous Metabolite, Protein, Lipid Extraction (SIMPLEX): A Combinatorial Multimolecular Omics Approach for Systems Biology. Mol. Cell. Proteomics *15*, 1453–1466. https://doi.org/10.1074/mcp.M115.053702.

100. El Abiead, Y., Bueschl, C., Panzenboeck, L., Wang, M., Doppler, M., Seidl, B., Zanghellini, J., Dorrestein, P.C., and Koellensperger, G. (2022). Heterogeneous multimeric metabolite ion species observed in LC-MS based metabolomics data sets. Anal. Chim. Acta *1229*, 340352. https://doi.org/10.1016/j.aca.2022.340352.

101. Hildebrandt, A., Bickmeyer, I., and Kühnlein, R.P. (2011). Reliable Drosophila Body Fat Quantification by a Coupled Colorimetric Assay. PLoS One *6*, e23796. https://doi.org/10.1371/journal.pone.0023796.

102. Xu, Y., Borcherding, A.F., Heier, C., Tian, G., Roeder, T., and Kühnlein, R. P. (2019). Chronic dysfunction of Stromal interaction molecule by pulsed RNAi induction in fat tissue impairs organismal energy homeostasis in Drosophila. Sci. Rep. *9*, 6989. https://doi.org/10.1038/s41598-019-43327-y.

103. Quarta, C., Fisette, A., Xu, Y., Colldén, G., Legutko, B., Tseng, Y.-T., Reim, A., Wierer, M., De Rosa, M.C., Klaus, V., et al. (2019). Functional identity of hypothalamic melanocortin neurons depends on Tbx3. Nat. Metab. *1*, 222–235. https://doi.org/10.1038/s42255-018-0028-1.

STAR★METHODS

KEY RESOURCES TABLE

REAGENT or RESOURCE	SOURCE	IDENTIFIER
Experimental models: Organisms/strains		
D.mel/Canton-S	Bloomington DSC	FBst0064349
D.mel/v^1y^1	Bloomington DSC	FBst0001509
D.mel/UAS-AdgfA-RNAi	Vienna DRC	FBst0469028
D.mel/LPP-Gal4 (fat body)	Gift from Irene Miguel-Aliaga	N/A
D.mel/HE-Gal4 (hemocytes)	Bloomington DSC	FBst0008699
D.mel/UAS-AdgfC-RNAi	Bloomington DSC	FBst0042915
D.mel/UAS-AdgfD-RNAi	Bloomington DSC	FBst0056980
D.mel/UAS-AdoR-RNAi (1)	Bloomington DSC	FBst0056866
D.mel/UAS-AdoR-RNAi (2)	Bloomington DSC	FBst0027536
D.mel/UAS-AdoR-RNAi (3)	Vienna DRC	FBst0451185
D.mel/Repo-Gal4 (pan-glia)	Bloomington DSC	FBst0007415
D.mel/nSyb-Gal4 (pan-neuron)	Bloomington DSC	FBst0051635
D.mel/Tdc2-Gal4 (OANs)	Bloomington DSC	FBst0009313
D.mel/TH,GMR58E02-Gal4 (DANs)	Siju et al. 2020	N/A
D.mel/TubP-Gal80^{TS}	Bloomington DSC	FBst0007019
D.mel/GMR85G01-Gal4 (PNG)	Bloomington DSC	FBst0040436
D.mel/GMR54C07-Gal4 (SPN)	Bloomington DSC	FBst0050472
D.mel/GMR86E01-Gal4 (ALG)	Bloomington DSC	FBst0045914
D.mel/GMR56F03-Gal4 (ENG)	Bloomington DSC	FBst0039157
D.mel/GMR54H02-Gal4 (CG)	Bloomington DSC	FBst0045784
D.mel/UAS-CaMPARI2-L398T	Bloomington DSC	FBst0078319
D.mel/UAS-CsChrimson-Venus	Bloomington DSC	FBst0055134
D.mel/LexAop-CsChrimson-tdTomato	Bloomington DSC	FBst0082183
D.mel/GMR85G01-LexA (PNG)	Bloomington DSC	FBst0054285
D.mel/GMR77A03-LexA (CG)	Bloomington DSC	FBst0054108
D.mel/UAS-GCaMP6f	Bloomington DSC	FBst0042747
D.mel/GMR58E02-LexA (PAM)	Bloomington DSC	FBst0052740
D.mel/LexAop-GCaMP7f	Bloomington DSC	FBst0080910
D.mel/UAS-rutabaga-RNAi	Bloomington DSC	FBst0080468
D.mel/UAS-NorpA-RNAi	Bloomington DSC	FBst0031113
Software and algorithms		
GraphPad Prism 10	GraphPad Software	https://www.graphpad.com/
ImageJ v1.8.0	NIH	https://imagej.nih.gov/ij/
Python 2.7 and 3.13	Python	https://www.python.org
Igor Pro 9	Wave Metrics	https://www.wavemetrics.com/
LAS AF	Leica Microsystems	https://www.leica-microsystems.com/
Analyst 1.7.2	AB Sciex	https://sciex.com/
ScanImage 2023.0.0	Pologruto et al.[95]	https://scanimage.org/

EXPERIMENTAL MODEL AND STUDY PARTICIPANT DETAILS

Flies were raised on standard cornmeal food under 12:12 h light/dark cycle at 25°C and 60% humidity. For starvation experiments, flies were transferred to a starvation vial containing a wet tissue paper as water source 24 h prior experiments. For pharmacological activation of AdoR, adult flies were kept on 2-chloradenosine supplemented food (2 mM; Sigma-Aldrich 861863) for 5 days prior experiments.[43] To allow Gal4-mediated transcription using the GeneSwitch system, adult flies were kept on RU486 (Sigma-Aldrich

M8046) supplemented food for 5 days prior starvation and experiment. An RU486 10 mM stock solution was first prepared in DMSO and subsequently diluted in melted fly food to achieve a final concentration of 200 μM.[54] For optogenetic experiments, adult flies were collected after hatching and kept on all *trans*-retinal supplemented food (1:250) under blue light only conditions. All experiments were conducted on 5-8-day old female flies, unless stated elsewhere.

METHOD DETAILS

FlyPAD feeding assay

FlyPAD feeding experiments were performed as previously described.[44] Single flies were transferred into the behavioral arena by mouth aspiration and left to feed for 1 h on two 5μL drops of low-temperature melting agarose (1.5%) supplemented with 10% sucrose. Experiments were conducted in a climate chamber where a temperature of 25°C and 60% humidity were maintained. For optogenetic genetic experiments, we used the closed-loop stimulation paradigm described by Moreira et al.[65] In this system, CsChrimson was activated by red light (625nm; 30μW/mm^2) for a continuous period of 10 s when the fly's proboscis contacted the drop of sucrose. Capacitance signal analysis was conducted using a custom-made MATLAB script provided by Pavel Itskov. The structure of feeding behavior was analyzed following the same parameters as described before[44] (Figure 1B). The cumulated and total number of sips, number of activity bouts and number of feeding bursts were summed for the two electrodes. The sip durations, inter-sips intervals, durations of activity bouts and durations of feeding bursts were averaged for the two electrodes.

Spherical treadmill behavioral assay

Single fly experiments on the spherical treadmill were performed using the same device and paradigm as previously described.[46] Briefly, the experimental fly was anesthetized on ice and tethered by gluing a tungsten pin on their thorax using UV-cured clue. Another drop of glue was used to glue the posterior part of the head to anterior part of the thorax and the wings were clipped. The fly was then immediately transferred onto the treadmill and was given 3 min of acclimatization before experiment initialization. Each trial consisted in pre-stimulation (20s), stimulation with balsamic vinegar odor (4ppm; 12s) and post-stimulation periods (30s; Figure 2I). The 10 consecutive recorded trials were separated by semi-randomized inter-trial periods of 60 ± 2–20 s. Data acquisition an analysis were performed using custom-written Python 2.7 scripts, as previously described.[46] For analysis, we measured the average running speed of the fly on the spherical treadmill during the 12s of odor stimulation.

CApillary FEeder (CAFE) assay

CAFE assay were performed as previously described with the following modifications.[96,97] Standard starvation vials were used as CAFE chambers. One glass graduated microcapillary (#022.7142, CAMAG, Muttenz, Switzerland) was pocked in through the vial plug and filled with 5 μL of sucrose solution (5% in water) supplemented with the food dye Allura Red AC (0.2%; Sigma-Aldrich, #458848) for visualization. Flies were tested by groups of 10 per CAFE chamber. For each experimental run, one vial was left without flies to account for liquid evaporation. CAFE chambers were then left over-night at 25°C and 60% humidity. The liquid decrease was measured after 16 h. Individual sucrose consumption was calculated by subtraction of the liquid decrease in the evaporation controls from the decrease measured in experimental vials and divided by the total number of flies. Vials where flies did not eat at all were excluded from further analysis. The different assays were conducted on a minimum of two experimental days using different batches of flies, for each genotype. The indicated "n" is the number of experimental CAFE vials.

Olfactory 4-arm maze

The 4-arm maze olfactory choice arena is a custom-made behavioral assay to monitor the preference behavior of freely moving adult flies upon olfactory stimulation and has been previously described.[97,98] In brief, groups of 15–20 24-h-starved female flies were left for 60 s in the arena for acclimatization. Then, the stimulus (vinegar, 10% in water) was delivered for 60 s in two opposite quadrants. Humidified air was used as control in the two other quadrants. After an inter-stimulus phase of 60 s, the stimulus was again delivered for 60 s in the two remaining quadrants. Behavior was monitored with an infrared camera (Flea3 USB3 1.3MP Mono, FLIR Systems), the background illumination being provided by infrared LEDs. Behavioral attraction toward vinegar odor was determined by calculating a preference index (PI): (number of flies in stimulus quadrants – number of flies in non-stimulus quadrants)/total number of flies. The indicated "n" is the number of experimental runs for each genotype.

Survival analysis

Groups of 50 female flies of each genotype were transferred into starvation vials and kept at 25°C and 60% humidity for 60–72 h. Dead flies were counted every 2nd hour during the day.

Adenosine content

Metabolite extraction

10 frozen flies per sample were transferred into Precellys tubes prefilled with ceramic beads (hard tissue lysing kit, CK28-R) and 1mL of −20°C MeOH:H_2O (4:1, v/v) was added to each sample. The homogenization was performed with a Precellys Evolution tissue homogenizer connected to a Cryolys module. The temperature was maintained at 4°C while 4 homogenization cycles where performed

at 7500 rpm for 20 s with 30 s break intervals. Next, homogenates were transferred into Eppendorf tubes, incubated for 15 min at 4°C and 950 rpm and finally centrifuged for 15 min at 15,500 rpm and 4°C. The recovered supernatant was dried under a gentle nitrogen flow. Each sample was reconstituted in 50 μL AcN/H_2O (9:1, v/v), briefly sonicated and centrifuged before LC separation.

LC-MS/MS analysis

Analysis of adenosine was performed as previously described with minor modifications.[99,100] Briefly, a Vanquish Flex UHPLC system (Thermo Fisher Scientific, Germering, Germany) was equipped with a fitted iHILIC-(P) Classic (2.1 × 100 mm, 5 μm) column and pre-column (20 × 2.1 mm, 5 μm, 200 Å; both Dichrom, Haltern am See, Germany). The mobile phases were 15 mM ammonium acetate in H_2O at pH = 9.4 (A) and 100% acetonitrile (B). Separation was achieved with the following gradient: 0 to 12 min ramp from 90% B to 26% B, 12 to 14 min 26% B, 14 to 17 min ramp to 10% B, 17 to19 min 10% B, 19 to 19.1 min ramp back to 90% B and equilibrate until min 27. 5 μL of each sample were injected onto the column twice (spiked/not spiked with an isotopically labeled adenosine standard (Eurisotop) and the LC separation was carried out at 40°C with a flow rate of 200 μL/min.

The LC system was coupled to a QTRAP 6500+ (Applied Biosystems, Darmstadt, Germany). The measurements were performed in positive mode with the following ESI Turbo V ion source parameters: curtain gas: 30 arbitrary units; temperature: 350°C; ion source gas 1:40 arbitrary units; ion source gas 2:65 arbitrary units; collision gas: medium; ion spray voltage: 5500 V. For the selected reaction monitoring (SRM) mode Q1 and Q3 were set to unit resolution and CE was 27 V. Data were acquired with Analyst (version 1.7.2; AB Sciex) and Skyline (3) was used to visualize results and manually integrate signals.

TAG content

50 5-days old adult male flies were transferred to food vials containing either fly HFHS diet or normal fly food for 2 days, respectively. HFHS diet (∼20% fat, ∼12.5% sugar) consisted in: peanut butter 37%, coconut oil 1%, sucrose 7.5%, water 7.5%, standard fly food 45%, grape juice 2% and propionic acid 0.2% (v/v). To allow fly access to water and avoid them sticking to the HFHS diet during feeding, a portion of fly food was loaded on the top of 5mL agar (1% in water) in the vials. 5 male flies per replicate were collected and stored at −20°C for fly body fat content measurement. Fly body fat content was determined by normalizing triglyceride to protein content of fly homogenates: triglyceride by the coupled-colorimetric assay (T7532, Pointe Scientific[101]) and protein by Bicinchoninic acid assay (23225, Thermofisher Scientific), as previously described.[102,103]

Dye feeding assay

For colorimetric assessment of food consumption, groups of 8–10 24-h-starved female flies were left feeding in vials containing HFHS food supplemented with Allura Red AC (0.2%; Sigma-Aldrich, #458848) for 6 h. 1–2 tubes per genotype were left without dye and served as blank. After feeding, flies were anesthetized, collected in 1.5 mL microtubes, homogenized in 200 μL PBS, 1% Triton X- and centrifuged at 13,000 rpm for 1 min. Then, 100 μL of each supernatant was aliquoted to 96-well plate. Absorbance at 504 nm was measured on Infinite M200 PRO plate reader (Tecan). The mean absorbance of blank controls was subtracted for the absorbance in experimental samples.

Ex vivo calcium imaging

Fly brains were dissected in adult hemolymph-like saline (AHL; NaCl, 103mM; $NaHCO_3$, 26mM; KCl, 3mM; $CaCl_2$, 1.5mM; $MgCl_2$, 4mM; NaH_2PO_4, 1mM; TES, 5mM; D-Glucose, 10mM; Trehalose, 10mM). In experiments simulating the hemolymph of starved flies, D-Glucose and Trehalose were replaced by 20mM D-ribose to preserve osmolarity. A single dissected brain was then mounted caudal side up between a microscope glass slide and a coverslip using the same medium as for dissection and placed under an inverted Leica SP5 laser scanning confocal microscope. The photoconversion of CaMPARI2-L398T proteins expressed by glial cells was achieved by illuminating the sample for 30 s using the mercury lamp of the microscope and a 395/25nm filter through a 20x water immersion objective (NA 0.7). 512x512 pixel confocal stacks of approximately 20μm (CG) or 10μm (PNG) tick volume of tissue (Δz = 1μm) were taken directly after photoconversion using the same 20x objective and a 4x digital zoom. The signal-to-noise ratio was improved by averaging 4 lines scans. An additional 405nm excitation laser was used in combination with the 488nm laser while recording the green channel to preserve CaMPARI2-L398T photoconversion.[59] Both CG and PNG were imaged on the dorso-caudal part of a randomly selected brain hemisphere, where the calyx of the MB is clearly identifiable.

For pharmacological stimulation of AdoR, the AdoR agonist 2-chloradenosine (Sigma-Aldrich 861863) was freshly diluted in AHL from a 10mM stock (in water) to achieve a final concentration of 10 μM, in the range of AdoR EC_{50}.[43] Directly after dissection, explant brains were transferred to 2-chloradenosine-containing saline (or control) and kept for 10 min before mounting and imaging.

Data were analyzed using ImageJ (NIH) by manual drawing ROIs on z-maximal projections of the confocal stacks. The ratio between the florescence intensities for the red and green channels were averaged between the ROIs for a single fly and compared between the different experimental conditions.

In vivo 2-photon calcium imaging

To record PAM-DAN responses to optogenetic stimulation of PNG and CG, respectively, we used the recombined TH,GMR58E02-Gal4 > UAS-GCaMP6f described in a previous study.[70] These flies were then crossed to GMR85G01-LexA (PNG) or GMR77A03-LexA (CG) > LexAop-CsChrimson-tdTomato flies, or to LexAop-CsChrimson-tdTomato flies without LexA driver as genetic controls.

To record PAM-DAN responses to vinegar odor in flies with knockdown of AdoR in glia we used the following genotypes: GMR58E02-LexA > LexAop-GCaMP7f; "glia"-Gal4 > UAS-AdoR-RNAi. The different glia Gal4 driver lines were the same as for our behavioral experiments. Flies carrying the UAS-AdoR-RNAi construct were used as genetic controls.

For *in vivo* imaging, flies were prepared as previously described.[70] In this preparation, the fly's body was restrained in a truncated 1mL pipette tip, impairing its movements. After dissection of the head cuticle, fat body and tracheae, the exposed brain was covered by a drop of low-temperature melting agarose diluted in the recording AHL to prevent brain movements. Fed flies were recorded using standard AHL (NaCl, 103mM; $NaHCO_3$, 26mM; KCl, 3mM; $CaCl_2$, 1.5mM; $MgCl_2$, 4mM; NaH_2PO_4, 1mM; TES, 5mM; D-Glucose, 10mM; Trehalose, 10mM), while starved flies were recorded using a solution depleted in D-Glucose and Trehalose (NaCl, 103mM; $NaHCO_3$, 26mM; KCl, 3mM; $CaCl_2$, 1.5mM; $MgCl_2$, 4mM; NaH_2PO_4; 1mM, TES, 5mM; D-ribose, 20mM).

CCaMP6f and GCaMP7f fluorescence signal was recorded on a Rapp OptoElectronic customized Sutter Instrument MOM 2-photon microscope equipped with a 25x Nikon water immersion objective (NA 1.10), 8kHz RGG resonant scanner, a fast z-piezo and a Hammamatsu gateable PMT. Excitation light was provided by a 920mm Toptica photonics laser. Stacks comprising the axons terminals of the PAM neurons innervating the horizontal lobe of the mushroom body were imaged at a frequency of 3 Hz (512x512 pixels; digital zoom 4x; 10 slices; $\Delta z = 5\mu m$) for optogenetic experiments or 2.31 Hz (512x512 pixels; digital zoom 4x; 13 slices; $\Delta z = 4\mu m$) for vinegar odor stimulation experiments.

Optogenetic stimulation was achieved using a 590 nm LED imbed in the microscope light-path. The light pulses were generated using an optical shutter (Uniblitz DSS25B) controlled via the SysCon2 (2.4.1) software (Rapp OptoElectronic). CsChrimson was activated in glia for 100 ms with an intensity of 8 $\mu W/mm^2$.

Vinegar-odor stimulation (1% in water) was delivered through a Syntech stimulus controller CS-55. During the entire duration of the experiment, flies were exposed to a continuous air flow (1 mL/min). Flies were stimulated for 12 s after a baseline recording of 30 s, to match with our spherical treadmill paradigm.

For analysis, ROIs delimiting the different lobes of the mushroom body ($\beta 2$, $\beta'2$, $\gamma 3$, 4 and 5) were manually drown using ImageJ (NIH) on a maximum z-projection of the imaged stacks, for each trial. Raw traces were then analyzed using custom Python3.0 scripts. For $\beta 2$, $\beta'2$ and $\gamma 4$ compartments, relative GCaMP fluorescence intensities ($\Delta F/F_0$) were computed using the averaged fluorescence intensity for the 5 frames preceding the stimulus presentation (F_0). The vinegar-response peak was defined as the maximal $\Delta F/F_0$ value measured during the stimulus phase. Since the $\gamma 3$ and 5 compartments did not show a clear baseline but rather an oscillatory pattern of activity, we calculated the basal fluorescence (F_0) by averaging the fluorescence intensity over the entire trial recording. The vinegar response and spontaneous peaks were defined as the difference between the maximal $\Delta F/F_0$ value measured during the stimulus phase and the minimal $\Delta F/F_0$ value measured directly before stimulation.

QUANTIFICATION AND STATISTICAL ANALYSIS

Results are expressed as the mean ± SEM or as a scatterplot displaying the individual data point as well as their mean ± SEM. The normality of data distributions was tested using the D'Agostino and Pearson test prior assessing significance. Two samples datasets significance was tested using Mann-Whitney U-test (non-normal distribution), Welch's t test (unequal SDs) or standard t test (equal SDs). Three or more samples datasets significance was tested using Kruskal-Wallis test (non-normal distribution), Welch's ANOVA (unequal SDs) or standard one-way ANOVA (equal SDs) followed by *post hoc* multiple comparisons (Dunn's tests for non-normally distributed data or Dunnett's tests for normally distributed ones). Datasets involving more than one independent factor were analyzed using 2- or 3-way ANOVA, depending on the experimental design. Food-odor tracking over successive trials data were analyzed using 2-way repeated measures ANOVA followed by Sidak's multiple comparisons tests. Details related to sample sizes, statistical tests and post hoc pairwise comparisons used for statistical analysis are reported in the figure and figure legends. The reported sample sizes are the number of flies used for the given experiment, except for the measurements of adenosine and TAG content, CAFE and 4-arm maze experiments where the number of flies per replicate is stated. Statistical analysis was performed using GraphPad Prism 10. The significance threshold was set as p-value <0.05.

Cell Reports, Volume *44*

Supplemental information

Adenosine signaling in glia modulates metabolic state-dependent behavior in *Drosophila*

Jean-François De Backer, Thomas Karges, Julia Papst, Zeynep Nigar Pınar, Cristina Coman, Robert Ahrends, Yanjun Xu, Cristina García-Cáceres, and Ilona C. Grunwald Kadow

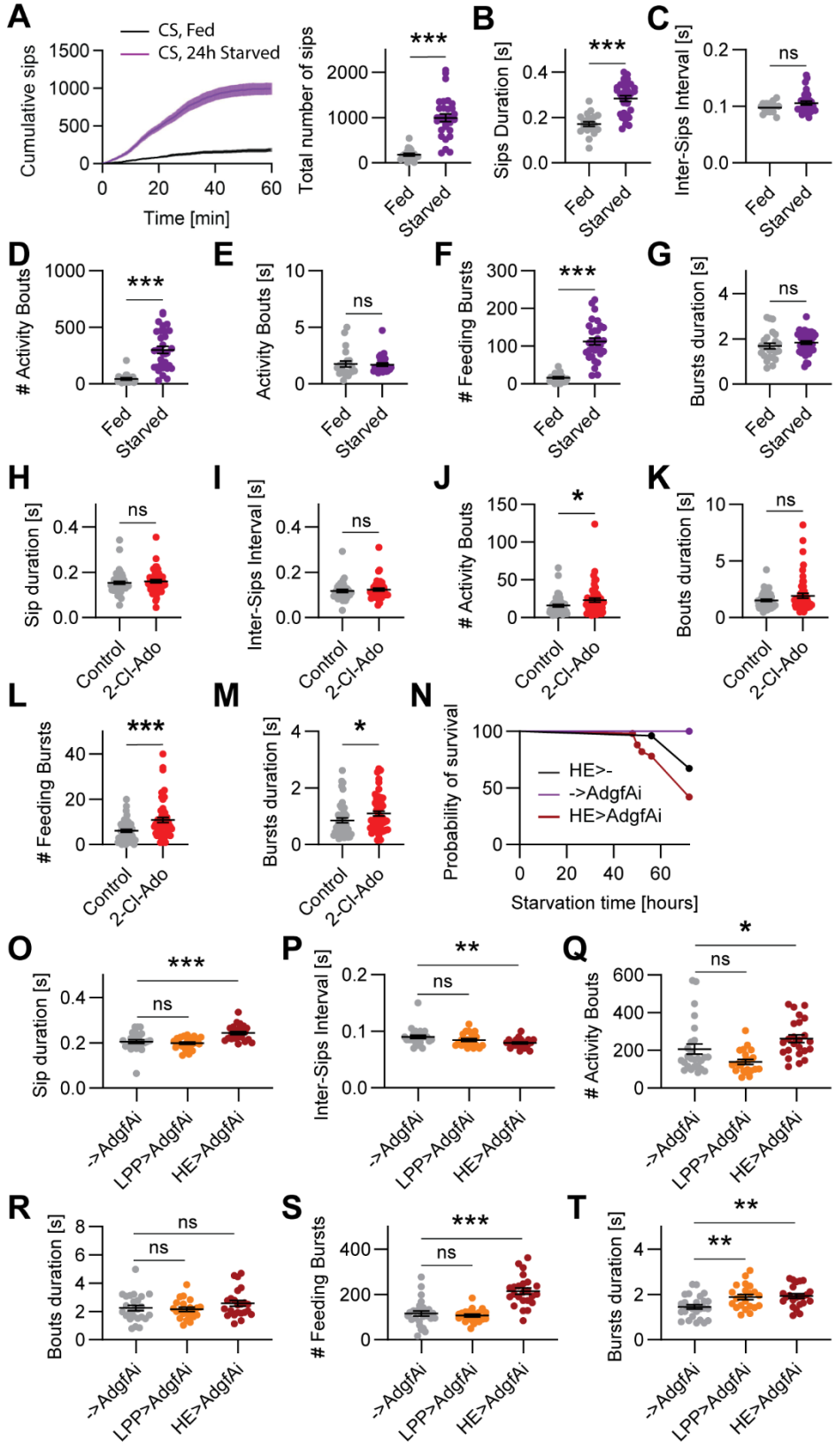
A
CS, Fed
CS, 24h Starved
Cumulative sips
Time [min]
Total number of sips
B
Sips Duration [s]
C
Inter-Sips Interval [s]
D
Activity Bouts
E
Activity Bouts [s]
F
Feeding Bursts
G
Bursts duration [s]
H
Sip duration [s]
I
Inter-Sips Interval [s]
J
Activity Bouts
K
Bouts duration [s]
L
Feeding Bursts
M
Bursts duration [s]
N
Probability of survival
HE>-
->AdgfAi
HE>AdgfAi
Starvation time [hours]
O
Sip duration [s]
P
Inter-Sips Interval [s]
Q
Activity Bouts
R
Bouts duration [s]
S
Feeding Bursts
T
Bursts duration [s]
Fed
Starved
Control
2-Cl-Ado
->AdgfAi
LPP>AdgfAi
HE>AdgfAi
ns

Figure S1: Extracellular adenosine modifies flies' feeding pattern similarly to starvation (related to Figure 1)

(A) Cumulative number of sips (mean ± SEM) and scatter plot of the total number of sips on 10% sucrose drops in fed and 24-h-starved CS flies in one hour (n = 29/45; Mann-Whitney test $p < 0.0001$). (B) Averaged sip duration (Mann-Whitney test $p < 0.0001$). (C) Averaged time interval between sips (Mann-Whitney test $p = 0.09$). (D) Total number of activity bouts (Mann-Whitney test $p < 0.0001$). (E) Averaged duration of activity bouts (Mann-Whitney test $p = 0.31$). (F) Total number of feeding bursts (Mann-Whitney test $p < 0.0001$). (G) Averaged duration of feeding bursts (Mann-Whitney test $p = 0.13$).

(H) Averaged sip duration in fed WT flies kept for 5 days on standard fly food supplemented with the AdoR agonist 2-chloroadenosine (2-Cl-Ado; 1.65 mM; n = 57/57; Mann-Whitney test $p = 0.29$). (I) Averaged time interval between sips (Mann-Whitney test $p = 0.43$). (J) Total number of activity bouts (Mann-Whitney test $p = 0.0179$). (K) Averaged duration of activity bouts (Mann-Whitney test $p = 0.37$). (L) Total number of feeding bursts (Mann-Whitney test $p = 0.0006$). (M) Averaged duration of feeding bursts (Mann-Whitney test $p = 0.0182$).

(N) Survival curves over 72 h of starvation for control flies (HE>- and ->AdgfAi) or upon knockdown of AdgfA in hemocytes (HE>AdgfAi; n = 50/50/50; Log-rank test $p < 0.0001$).

(O) Averaged sip duration in 24-h-starved control flies (->AdgfAi) or upon knockdown of AdgfA in the fat body (LPP>AdgfAi) or hemocytes (HE>AdgfAi; n = 25/22/24; Kruskal-Wallis test $p = 0.0002$). (P) Averaged time interval between sips (Kruskal-Wallis test $p = 0.0056$). (Q) Total number of activity bouts (Kruskal-Wallis test $p < 0.0001$). (R) Averaged duration of activity bouts (one-way ANOVA $p = 0.25$). (S) Total number of feeding bursts (Kruskal-Wallis test $p < 0.0001$). (T) Averaged duration of feeding bursts (one-way ANOVA $p = 0.0017$).

Scatter plots display individual data points, as well as the mean ± SEM for each group. Pair-wise comparisons are indicated as follow: ns, non-significant ($p > 0.05$); *, $p < 0.05$; **, $p < 0.01$; *** $p < 0.001$.

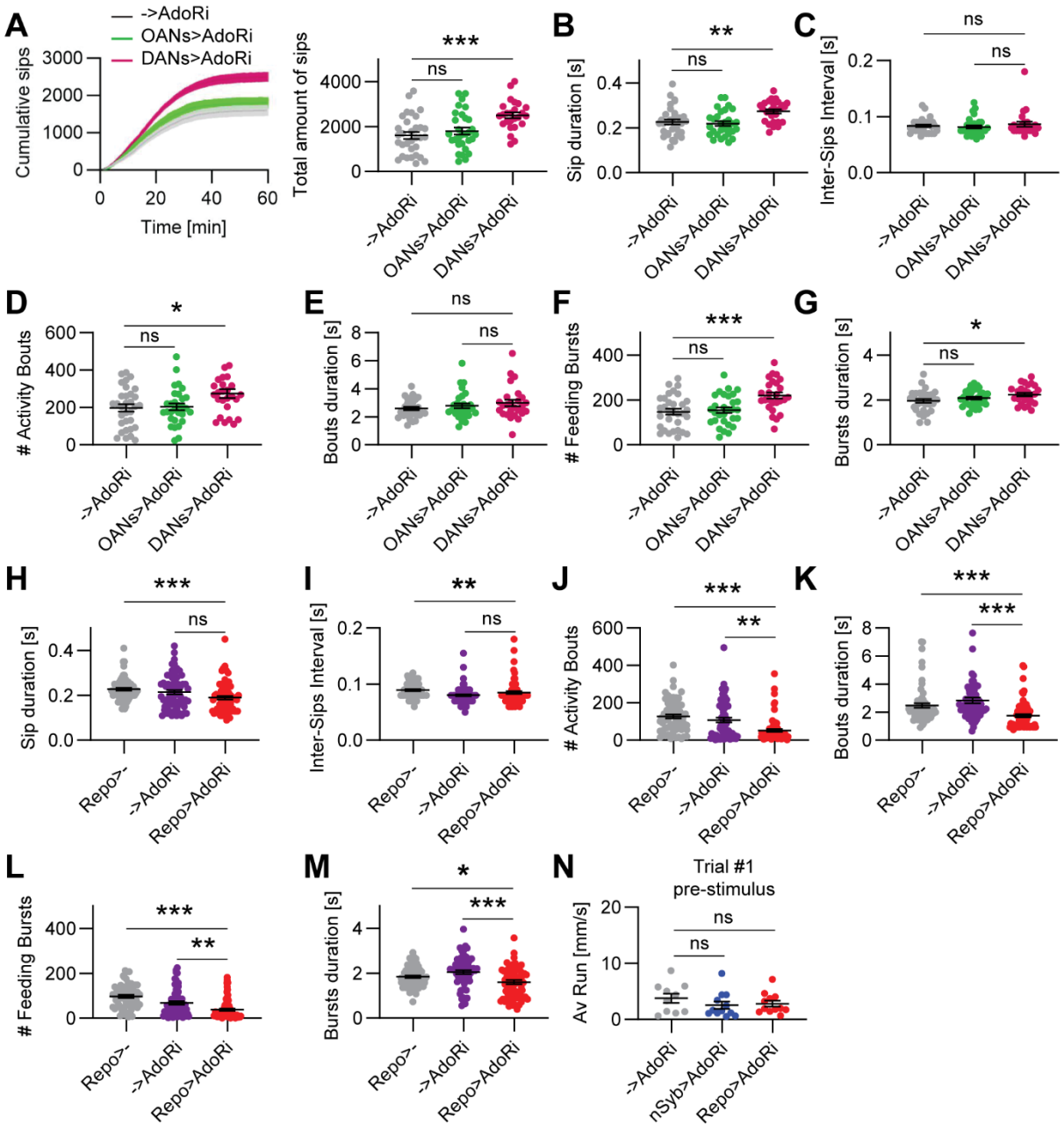

Figure S2: Adenosine signaling in dopaminergic neurons inhibits feeding behavior (related to Figure 2)

(A) Cumulative number of sips (mean ± SEM) and scatter plot of the total number of sips on 10% sucrose drops in 24-h-starved control flies (->AdoRi) or upon knockdown of AdoR in octopaminergic (OANs>AdoRi) and dopaminergic neurons (DANs>AdoRi; n = 32/30/25; one-way ANOVA p = 0.0002). (B) Averaged sip duration (one-way ANOVA p = 0.0002). (C) Averaged time interval between sips (Kruskal-Wallis test p = 0.39). (D) Total number of activity bouts (Kruskal-Wallis test p = 0.0272). (E) Averaged duration of activity bouts (Kruskal-Wallis test p = 0.43). (F) Total number of feeding bursts (one-way ANOVA p = 0.0004). (G) Averaged duration of feeding bursts (one-way ANOVA p = 0.0437).

(H) Averaged sip duration in 24-h-starved control flies (Repo>- and ->AdoRi) or upon knockdown AdoR in glia (Repo>AdoRi; n = 20/20/32; Kruskal-Wallis test p=0.0003). (I) Averaged time interval between sips (Kruskal-Wallis test $p = 0.0001$). (J) Total number of activity bouts (Kruskal-Wallis test $p < 0.0001$). (K) Averaged duration of activity bouts (Kruskal-Wallis test $p < 0.0001$). (L) Total number of feeding bursts (Kruskal-Wallis test $p < 0.0001$). (M) Averaged duration of feeding bursts (Kruskal-Wallis test $p < 0.0001$).

(N) Average forward running speed during the pre-stimulus phase of the 1st trial in 24-h-starved control (->AdoRi) flies or upon knockdown of AdoR in neurons (nSyb>AdoRi) and glia (Repo>AdoRi), respectively (n = 10/12/12; Kruskal-Wallis test $p = 0.40$).

Scatter plots display individual data points, as well as the mean ± SEM for each group. Pair-wise comparisons are indicated as follow: ns, non-significant ($p > 0.05$); *, $p < 0.05$; **, $p < 0.01$; *** $p < 0.001$.

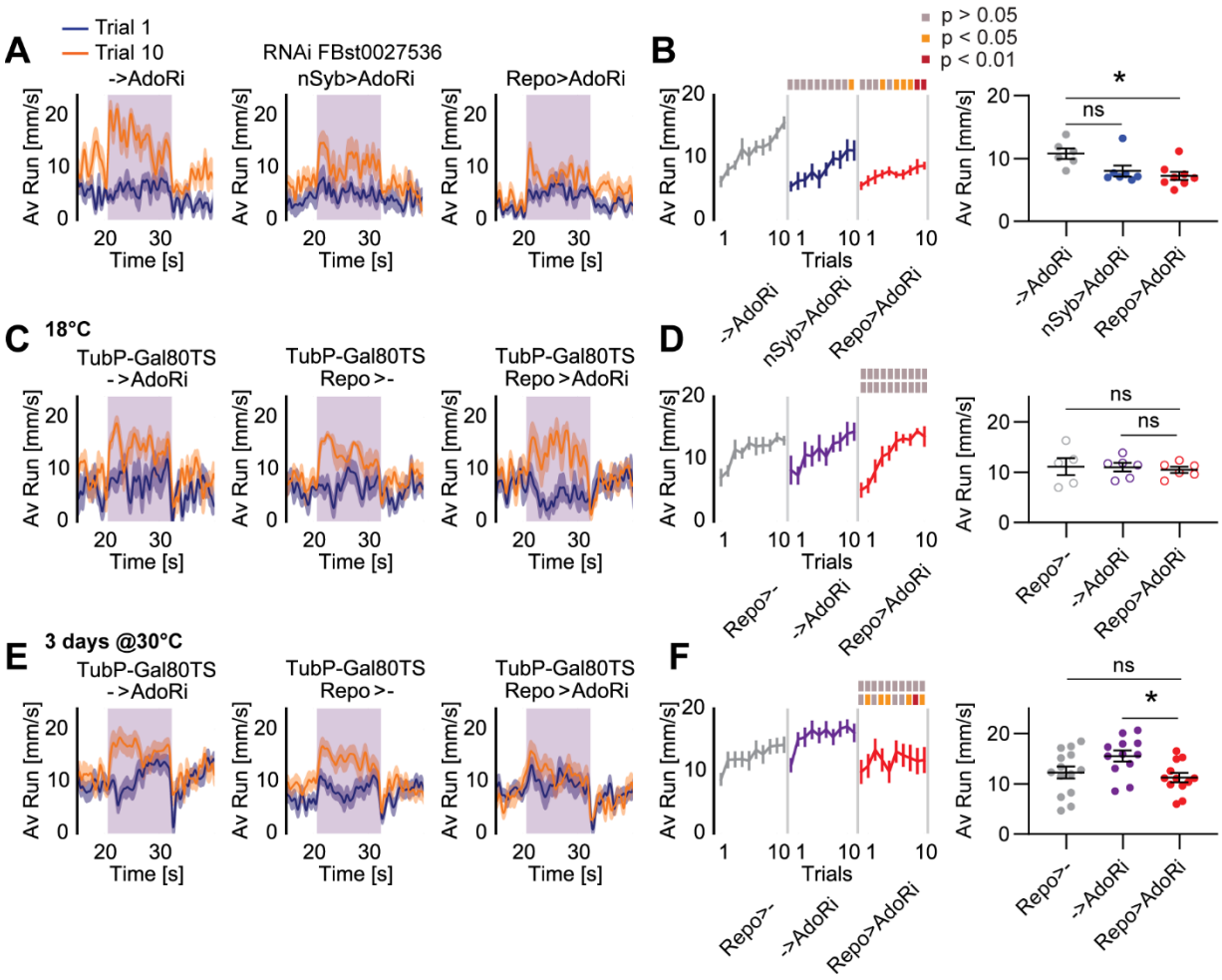

Figure S3: Adenosine signaling in glia is necessary for food-odor tracking behavior in adult flies (related to Figure 2)

(A) Averaged forward running speed (± SEM) in 24-h-starved control flies (->AdoRi) or upon knockdown of AdoR in neurons (nSyb>AdoRi) and glia (Repo>AdoRi) using an alternative RNAi line (FBst0027536), respectively. (B) Running speed during the stimulus phase over 10 successive trials (mean ± SEM; n = 6/7/8; 2-way RM ANOVA p(groups) = 0.0147; p(trials) < 0.0001; p(interaction) = 0.0830). The scatter plot displays the averaged running speed over the 10 trials for individual flies (Kruskal-Wallis test p = 0.0087). (C-F) Restriction of AdoR knockdown in adult flies using the temperature-sensitive TARGET system. (C) Averaged forward running speed (± SEM) in 24-h-starved control flies (TubP-Gal80^{TS}, Repo>- and TubP-Gal80^{TS}, ->AdoRi) or upon knockdown of AdoR in glia (TubP-Gal80^{TS}, Repo>AdoRi) in flies raised and kept at 18°C to prevent RNAi expression. (D) Running speed during the stimulus phase over 10 successive trials (mean ± SEM; n = 6/5/6; 2-way RM ANOVA p(groups) = 0.90; p(trials) < 0.0001; p(interaction) = 0.13). The scatter plot displays the averaged running speed over the 10 trials for individual flies (Kruskal-Wallis test p = 0.85). (E) Averaged forward running speed (± SEM) in 24-h-starved control flies (TubP-Gal80^{TS}, Repo>- and TubP-Gal80^{TS}, ->AdoRi) or upon knockdown of AdoR in glia (TubP-Gal80^{TS}, Repo>AdoRi) in flies raised at 18°C to prevent RNAi expression. Flies were kept for 2 days at 30°C before experiment to enable RNAi expression. (F) Running speed during the stimulus phase over 10 successive trials (mean ± SEM; n = 14/12/12; 2-way RM ANOVA p(groups) = 0.0275; p(trials) < 0.0001;

p(interaction) = 0.54). The scatter plot displays the averaged running speed over the 10 trials for individual flies (one-way ANOVA $p = 0.0275$).
Sidak's post hoc trial-to-trial comparisons are depicted on the top of the graphs as color-coded boxes (grey $p > 0.05$, orange $p < 0.05$ and red $p < 0.01$). Scatter plots display individual data points, as well as the mean ± SEM for each group. Pair-wise comparisons are indicated as follow: ns, non-significant ($p > 0.05$); *, $p < 0.05$; **, $p < 0.01$; *** $p < 0.001$.

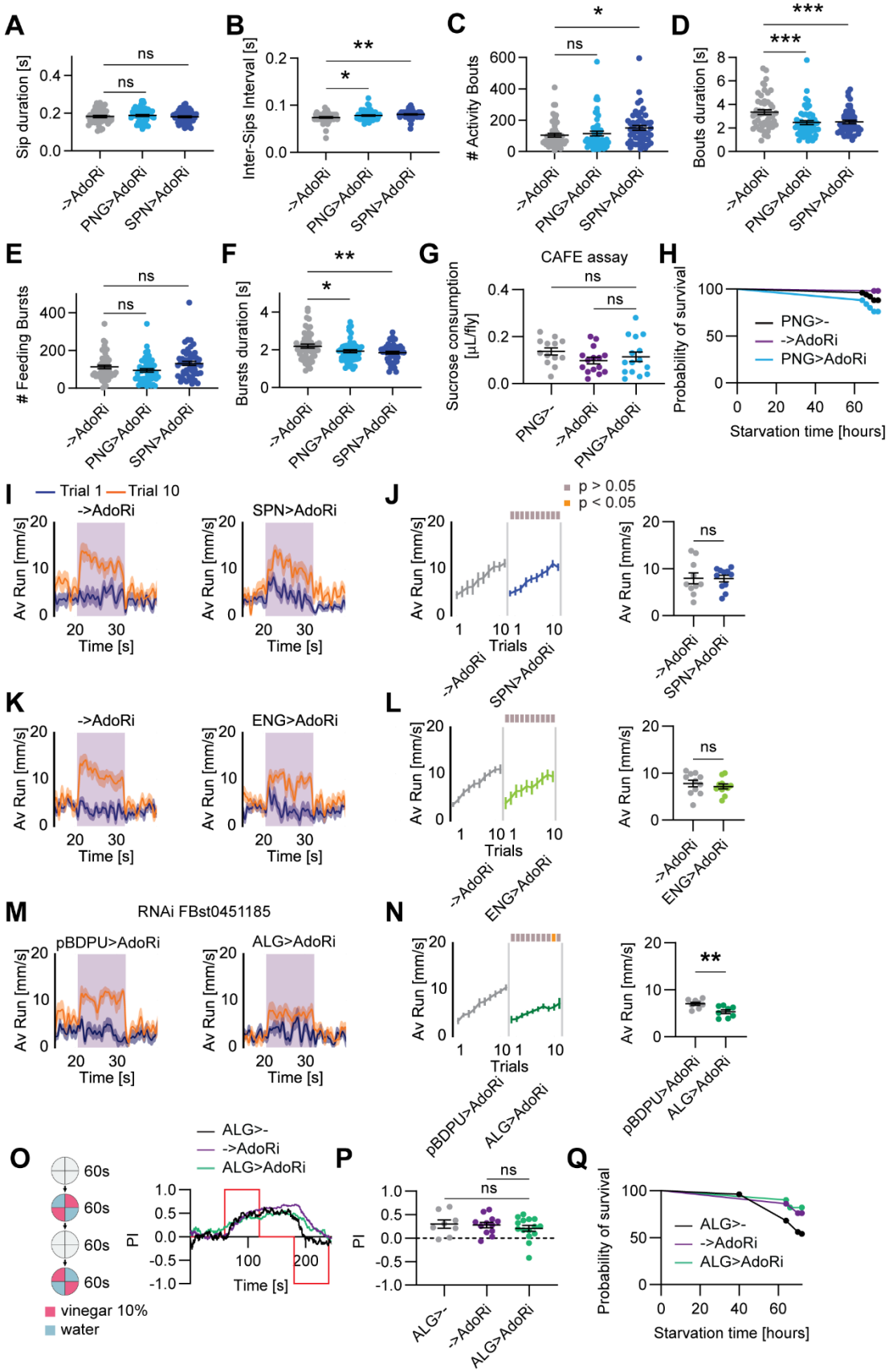
A
Sip duration [s]
ns
ns
->AdoRi
PNG>AdoRi
SPN>AdoRi
B
Inter-Sips Interval [s]
**
*
C
Activity Bouts
*
ns
D
Bouts duration [s]
***
***
E
Feeding Bursts
F
Bursts duration [s]
G
CAFE assay
Sucrose consumption [µL/fly]
PNG>-
H
Probability of survival
PNG>-
->AdoRi
PNG>AdoRi
Starvation time [hours]
I
Trial 1
Trial 10
Av Run [mm/s]
Time [s]
J
p > 0.05
p < 0.05
Trials
K
ENG>AdoRi
L
M
RNAi FBst0451185
pBDPU>AdoRi
ALG>AdoRi
N
O
60s
vinegar 10%
water
PI
Time [s]
P
Q

Figure S4: Adenosine signaling in subperineurial and ensheating glia is not necessary for food-odor tracking behavior (related to Figure 3)

(A) Averaged sip duration in 24-h-starved control flies (->AdoRi) or flies deficient for AdoR in PNG (PNG>AdoRi) and SPN (SPN>AdoRi), respectively (n = 49/51/48; one-way ANOVA p = 0.60). (B) Averaged time interval between sips (Kruskal-Wallis test p = 0.0013). (C) Total number of activity bouts (Kruskal-Wallis test p = 0.0117). (D) Averaged duration of activity bouts (Kruskal-Wallis test p = 0.0005). (E) Total number of feeding bursts (Kruskal-Wallis test p = 0.0270). (F) Averaged duration of feeding bursts (Kruskal-Wallis test p = 0.0481).

(G) Total sucrose consumption in control flies (PNG>- and ->AdoRi) or upon knockdown of AdoR in PNG (PNG>AdoRi) after 16h in the CAFE (n = 13/15/15; Kruskal-Wallis test p = 0.23).

(H) Survival curves over 72 h of starvation for control flies (PNG>- and ->AdoRi) or upon knockdown of AdoR in PNG (PNG>AdoRi; n = 50/50/50; Log-rank test p = 0.0036).

(I) Averaged forward running speed (± SEM) in 24-h-starved control flies (->AdoRi) or upon knockdown of AdoR in SPN (SPN>AdoRi) (J) Running speed during the stimulus phase over 10 successive trials (mean ± SEM; n = 10/11; 2-way RM ANOVA p(groups) = 0.98; p(trials) < 0.0001; p(interaction) = 0.85). The scatter plot displays the averaged running speed over the 10 trials for individual flies (Unpaired t-test p = 0.98).

(K) Averaged forward running speed (± SEM) in 24-h-starved control flies (->AdoRi) or upon knockdown of AdoR in ENG (ENG>AdoRi). (L) Running speed during the stimulus phase over 10 successive trials (mean ± SEM; n = 10/11; 2-way RM ANOVA p(groups) = 0.47; p(trials) < 0.0001; p(interaction) = 0.77). The scatter plot displays the averaged running speed over the 10 trials for individual flies, as well as their mean ± SEM (Unpaired t test p = 0.47).

(M) Averaged forward running speed (± SEM) in 24-h-starved control flies (pBDPU>AdoRi) or upon knockdown of AdoR in ALG (ALG>AdoRi) using an alternative RNAi line (FBst041185). (N) Running speed during the stimulus phase over 10 successive trials (mean ± SEM; n = 8/8; 2-way RM ANOVA p(groups) = 0.0070; p(trials) < 0.0001; p(interaction) = 0.0393). The scatter plot displays the averaged running speed over the 10 trials for individual flies (Unpaired t test p = 0.0070).

(O) Schematic representation of the experimental protocol used for 4-arm maze behavioral assay and average time course of preference indices (PI) during vinegar (10%) presentation for 24-h-starved control (ALG>- and ->AdoRi) flies or upon knockdown of AdoR in ALG (ALG>AdoRi). The red rectangles represent the stimulus presentations. (P) Averaged PIs during vinegar presentation (n = 8/12/15; Kruskal-Wallis test p = 0.80).

(Q) Survival curves over 72 h of starvation for control flies (ALG>- and ->AdoRi) or upon knockdown of AdoR in ALG (ALG>AdoRi; n = 50/50/50; Log-rank test p = 0.0041).

For food-odor tracking behavior experiments, Sidak's post hoc trial-to-trial comparisons are depicted on the top of the graphs as color-coded boxes (grey $p > 0.05$, orange $p < 0.05$ and red $p < 0.01$). Scatter plots display individual data points, as well as the mean ± SEM for each group. Post hoc pair-wise comparisons are indicated as follow: ns, non-significant ($p > 0.05$; *, $p < 0.05$; **, $p < 0.01$; *** $p < 0.001$.

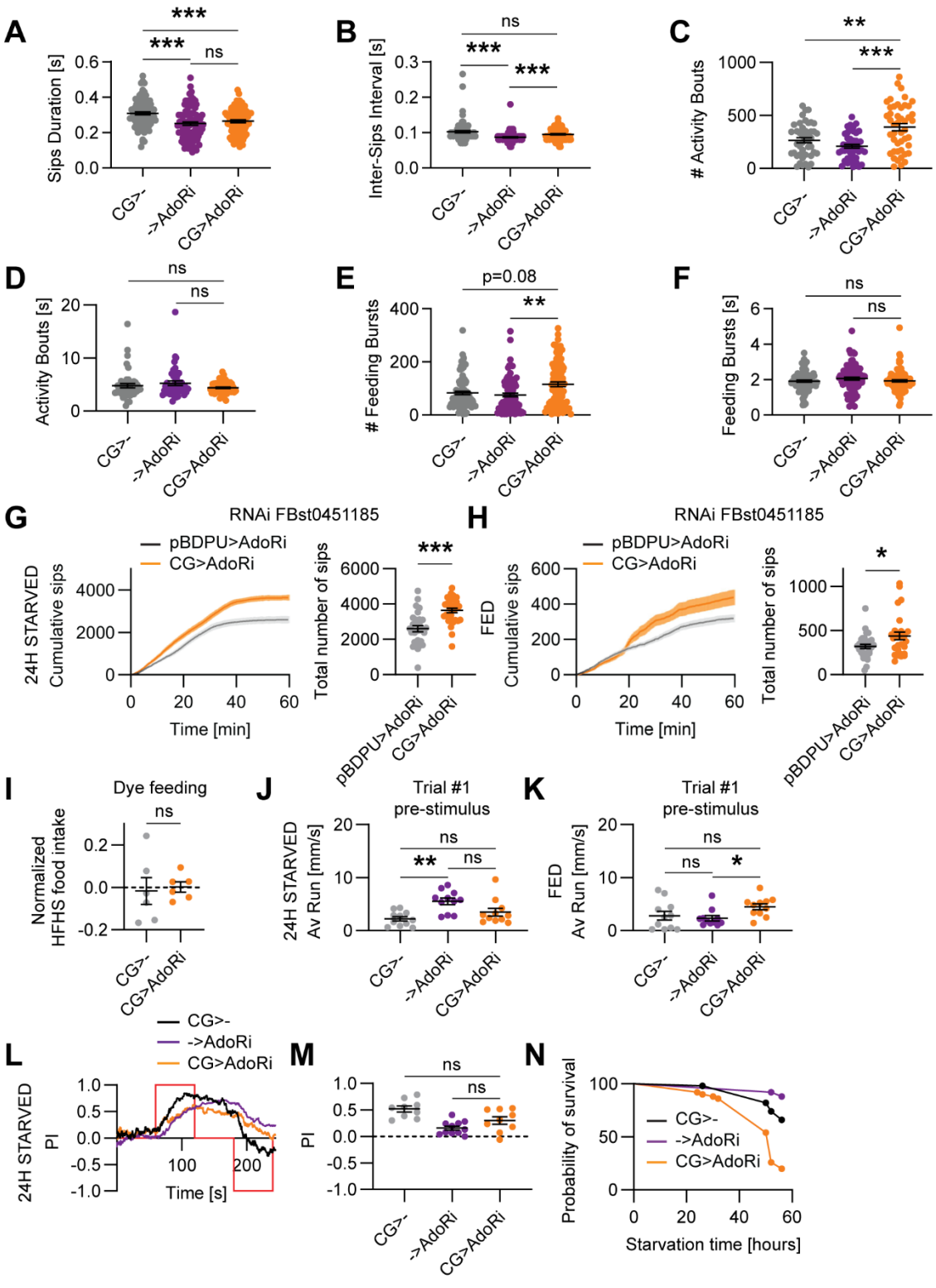

Figure S5: Adenosine signaling in cortex glia inhibits feeding and food-odor tracking behavior (Related to Figure 4)

(A) Averaged sip duration in 24-h-starved control flies (CG>- and ->AdoRi) or flies deficient for AdoR in CG (CG>AdoRi; n = 45/44/44; one-way ANOVA $p < 0.0001$). (B) Averaged time interval between sips

(Kruskal-Wallis test $p < 0.0001$). (C) Total number of activity bouts (Welch's ANOVA $p < 0.0001$). (D) Averaged duration of activity bouts (Kruskal-Wallis test $p = 0.53$). (E) Total number of feeding bursts (Kruskal-Wallis test $p = 0.0024$). (F) Averaged duration of feeding bursts (Kruskal-Wallis test $p = 0.18$).
(G) Cumulative number of sips (mean ± SEM) and scatter plot of the total number sips on 10% sucrose drops in 24-h-starved control flies (pBDPU>AdoRi) and AdoR-deficient flies in CG (CG>AdoRi) using an alternative RNAi line (FBst041185; $n = 29/30$; Unpaired t test $p < 0.0001$).
(H) Cumulative number of sips (mean ± SEM) and scatter plot of the total number sips on 10% sucrose drops in fed control flies (pBDPU>AdoRi) or AdoR-deficient flies in CG (CG>AdoRi) using an alternative RNAi line (FBst041185; $n = 32/28$; Mann Whitney test $p = 0.0406$).
(I) Normalized HFHS food intake measured by colorimetry in control flies (CG>-) and AdoR-deficient flies in CG (CG>AdoRi; $n = 6/6$; Mann Whitney test $p = 0.48$).
(J) Average forward running speed during the pre-stimulus phase of the 1st trial in 24-h-starved control (CG>- and ->AdoRi) flies or upon knockdown of AdoR in CG (CG>AdoRi; $n = 11/11/11$; Kruskal-Wallis test $p = 0.0046$).
(K) Average forward running speed during the pre-stimulus phase of the 1st trial in 24-h-starved control (CG>- and ->AdoRi) flies or upon knockdown of AdoR in CG (CG>AdoRi; $n = 11/11/11$; Kruskal-Wallis $p = 0.0323$).
(L) Average time course of preference indices (PI) during vinegar (10%) presentation for 24-h-starved control (CG>- and ->AdoRi) flies or upon knockdown of AdoR in CG (CG>AdoRi). The red rectangles represent the stimulus presentations. (M) Averaged PIs during vinegar presentation ($n = 9/11/9$; Kruskal-Wallis test $p = 0.0013$).
(N) Survival curves over 56 h of starvation for control flies (ALG>- and ->AdoRi) or upon knockdown of AdoR in ALG (ALG>AdoRi; $n = 50/50/50$; Log-rank test $p < 0.0001$).
Scatter plots display individual data points, as well as the mean ± SEM for each group. Post hoc pair-wise comparisons are indicated as follow: ns, non-significant ($p > 0.05$; *, $p < 0.05$; **, $p < 0.01$; *** $p < 0.001$.

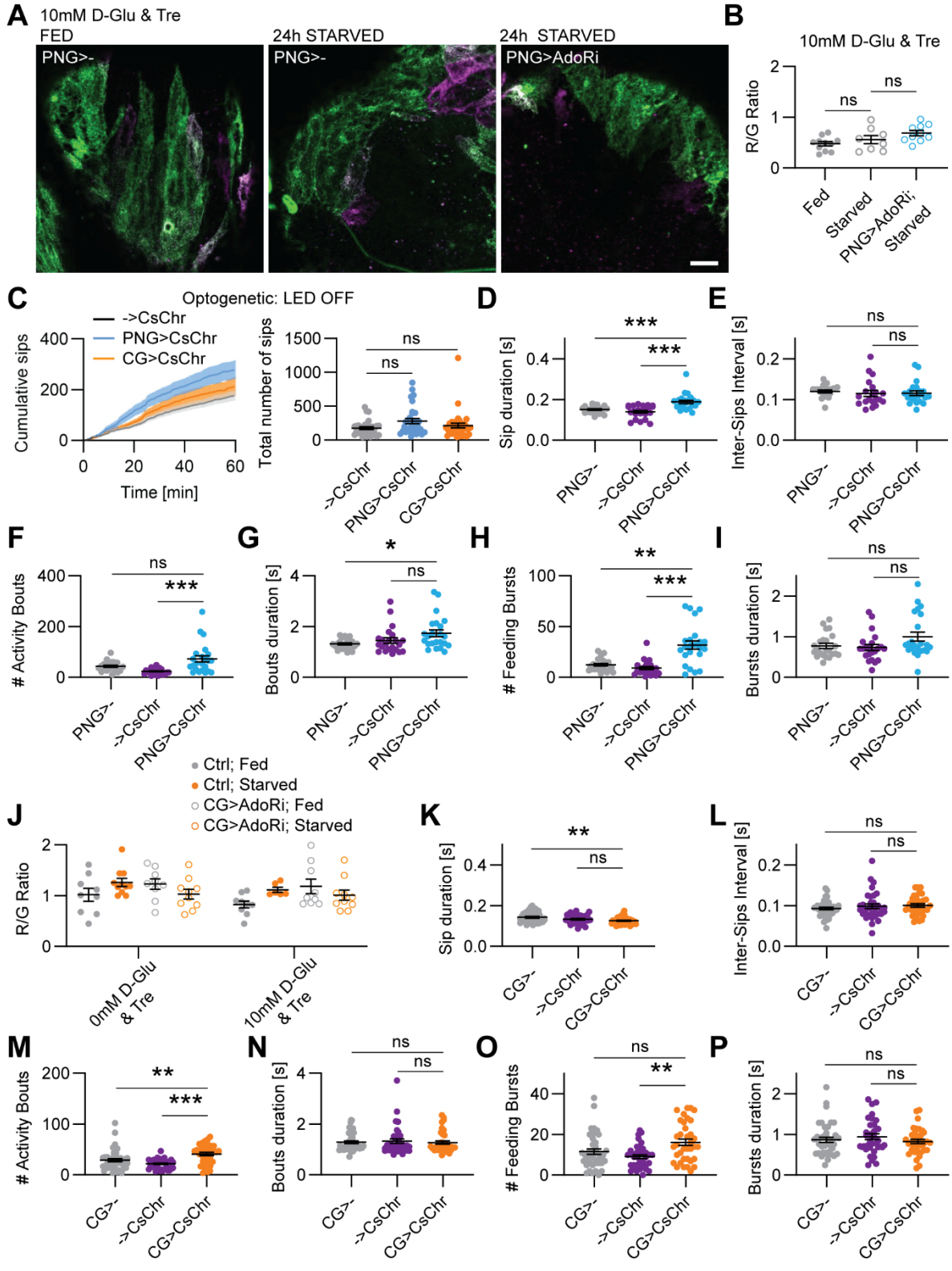

Figure S6: Starvation and adenosine signaling modulate intra-cellular calcium levels in perineurial and cortex glia (related to Figure 5)

(A) Example images of CaMPARI2-L398T-expressing PNG cells in dorso-caudal brain explants from fed and 24-h-starved control flies (PNG>-) and upon knockdown of AdoR (PNG>AdoRi), in standard AHL (10 mM D-Glu and 10 mM Tre), after photoconversion (scale bar = 20 µm). (B) CaMPARI2 photoconversion ratios in fed and 24-h-starved control flies (n = 11/8), as well as 24-h-starved PNG>AdoRi flies (n = 10; 2-way ANOVA p(AHL) = 0.0076; p(groups) = 0.06; p(interaction) = 0.06).
(C) Cumulative number of sips (mean ± SEM) and scatter plot of the total number sips on 10% sucrose drops in fed control flies (->CsChr) and flies expressing CsChrimson in PNG (PNG>CsChr) and CG (CG>CsChr), respectively, without light stimulation (n = 32/32/32; Kruskal-Wallis test p = 0.10).
(D) Averaged sip duration in fed flies upon closed-loop optogenetic activation of PNG (n = 23/22/23; Kruskal-Wallis test $p < 0.0001$). (E) Averaged time interval between sips (Kruskal-Wallis test p = 0.17). (F) Total number of activity bouts (Kruskal-Wallis test $p < 0.0001$). (G) Averaged duration of activity bouts (Kruskal-Wallis test p = 0.0283). (H) Total number of feeding bursts (Kruskal-Wallis test $p < 0.0001$). (I) Averaged duration of feeding bursts (Kruskal-Wallis test p = 0.10).
(J). CaMPARI2 photoconversion ratios in fed and 24-h-starved control and CG>AdoRi flies imaged in standard (n_{fed}=9/11; $n_{starved}$=9/10) or sugar-free AHL (n_{fed}=9/8; $n_{starved}$=9/10; 3-way ANOVA p(state) = 0.43; p(genotype) = 0.59; p(AHL) = 0.18; p(state x genotype) = 0.0022; p(state x AHL) = 0.35; p(genotype x AHL) = 0.79; p(state x genotype x AHL) = 0.95). Data from standard and sugar-free AHL are pooled for display in Figure 5F.
(K) Averaged sip duration in fed flies upon closed-loop optogenetic activation of CG (n = 44/41/37; one-way ANOVA p = 0.0037). (L) Averaged time interval between sips (Kruskal-Wallis test p = 0.48). (M) Total number of activity bouts (Kruskal-Wallis test $p < 0.0001$). (N) Averaged duration of activity bouts (Kruskal-Wallis test p = 0.85). (O) Total number of feeding bursts (Kruskal-Wallis test p = 0.0059). (P) Averaged duration of feeding bursts (Kruskal-Wallis test p = 0.62).
Scatter plots display individual data points, as well as the mean ± SEM for each group. Post hoc pair-wise comparisons are indicated as follow: ns, non-significant ($p > 0.05$); *, $p < 0.05$; **, $p < 0.01$; *** $p < 0.001$.

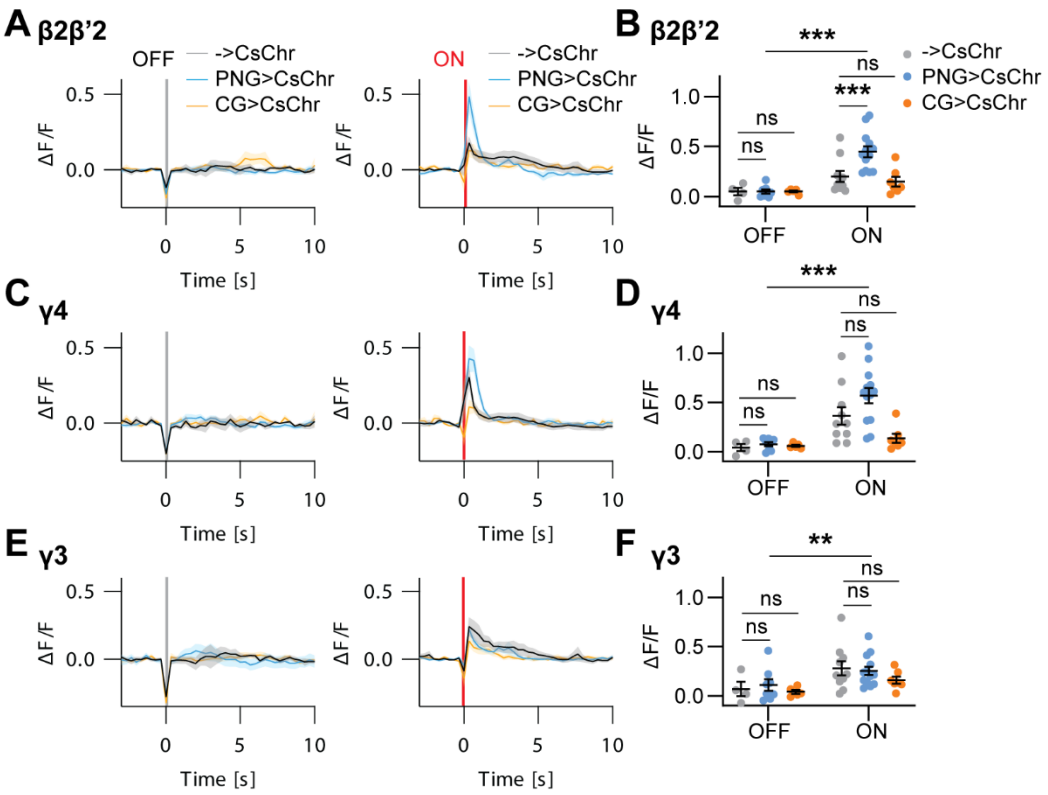

Figure S7: Optogenetic PNG stimulation evokes calcium transients in specific PAM dopaminergic neurons (related to Figure 5)

(A) Average (± SEM) ΔF/F calcium responses in PAM-DANs innervating the β2β'2 compartments of the MB to 100 ms optogenetic stimulation (*grey* line: LED OFF; *red* line: LED ON) of PNG (PNG>CsChr) and CG (CG>CsChr), respectively. (B) Calcium peak response following the stimulus (LED OFF: n = 4/8/5; LED ON n = 10/13/7; 2-way ANOVA p(genotype) = 0.0128; p(LED) < 0.0001; p(interaction) = 0.0122).

(C) Average (± SEM) ΔF/F calcium responses in PAM-DANs innervating the γ4 compartment of the MB to 100 ms optogenetic stimulation (*grey* line: LED OFF; *red* line: LED ON) of PNG (PNG>CsChr) and CG (CG>CsChr), respectively. (D) Calcium peak response following the stimulus (LED OFF: n = 4/8/5; LED ON n = 10/13/7; 2-way ANOVA p(genotype) = 0.0200; p(LED) < 0.0001; p(interaction) = 0.0364).

(E) Average (± SEM) ΔF/F calcium responses in PAM-DANs innervating the γ3 compartment of the MB to 100 ms optogenetic stimulation (*grey* line: LED OFF; *red* line: LED ON) of PNG (PNG>CsChr) and CG (CG>CsChr), respectively. (F) Calcium peak response following the stimulus (LED OFF: n = 4/8/5; LED ON n = 10/13/7; 2-way ANOVA p(genotype) = 0.37; p(LED) = 0.0037; p(interaction) = 0.77).

Scatter plots display individual data points, as well as the mean ± SEM for each group. Post hoc pair-wise comparisons are indicated as follow: ns, non-significant (p >0.05); *, p < 0.05; **, p < 0.01; *** p < 0.001.

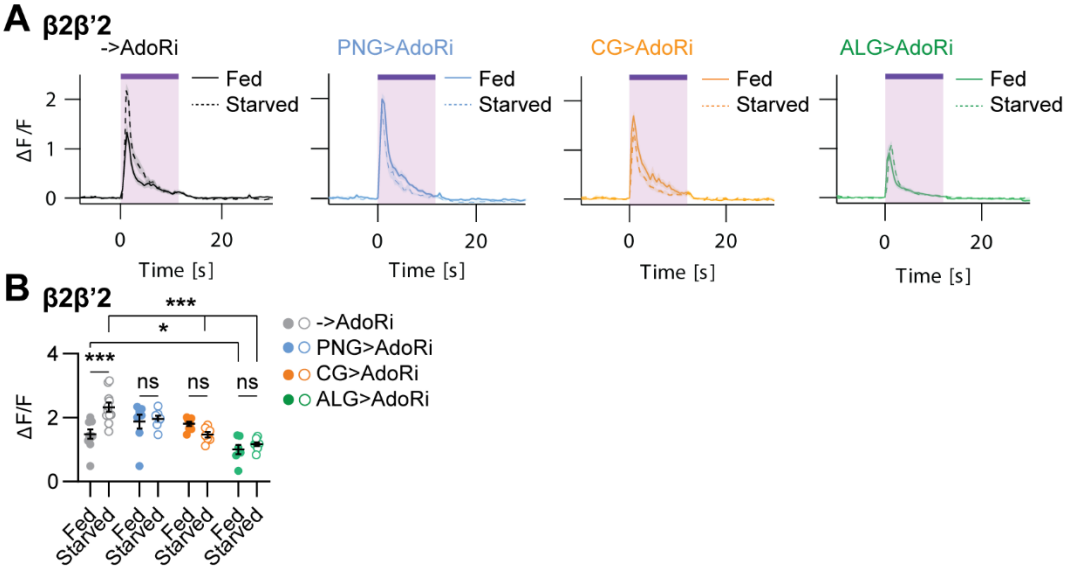

Figure S8: Adenosine signaling in perineurial, cortex and astrocyte-like glia differentially modulates PAM-β2β'2 dopaminergic neurons response to vinegar in fed and starved flies (related to Figure 7)
(A) Averaged ΔF/F calcium responses to vinegar-odor stimulation (*purple*) in the β2β'2 compartments in fed and 24-h-starved control flies (->AdoRi) or in flies expressing *AdoR*-RNAi in PNG (*blue*; PNG>AdoRi), CG (*orange*; CG>AdoRi) and ALG (*green*; ALG>AdoRi), respectively. (B) Maximal peak responses to vinegar-odor in the different groups ($n_{->AdoRi}$=10/11; $n_{PNG>AdoRi}$=8/7; $n_{CG>AdoRi}$=8/7; $n_{ALG>AdoRi}$ = 7/8; 2-way ANOVA p(genotype) < 0.0001, p(state) = 0.06, p(interaction) = 0.0004).
Scatter plots display individual data points, as well as the mean ± SEM for each group. Post hoc pair-wise comparisons are indicated as follow: ns, non-significant (p >0.05); *, p < 0.05; **, p < 0.01; *** p < 0.001.

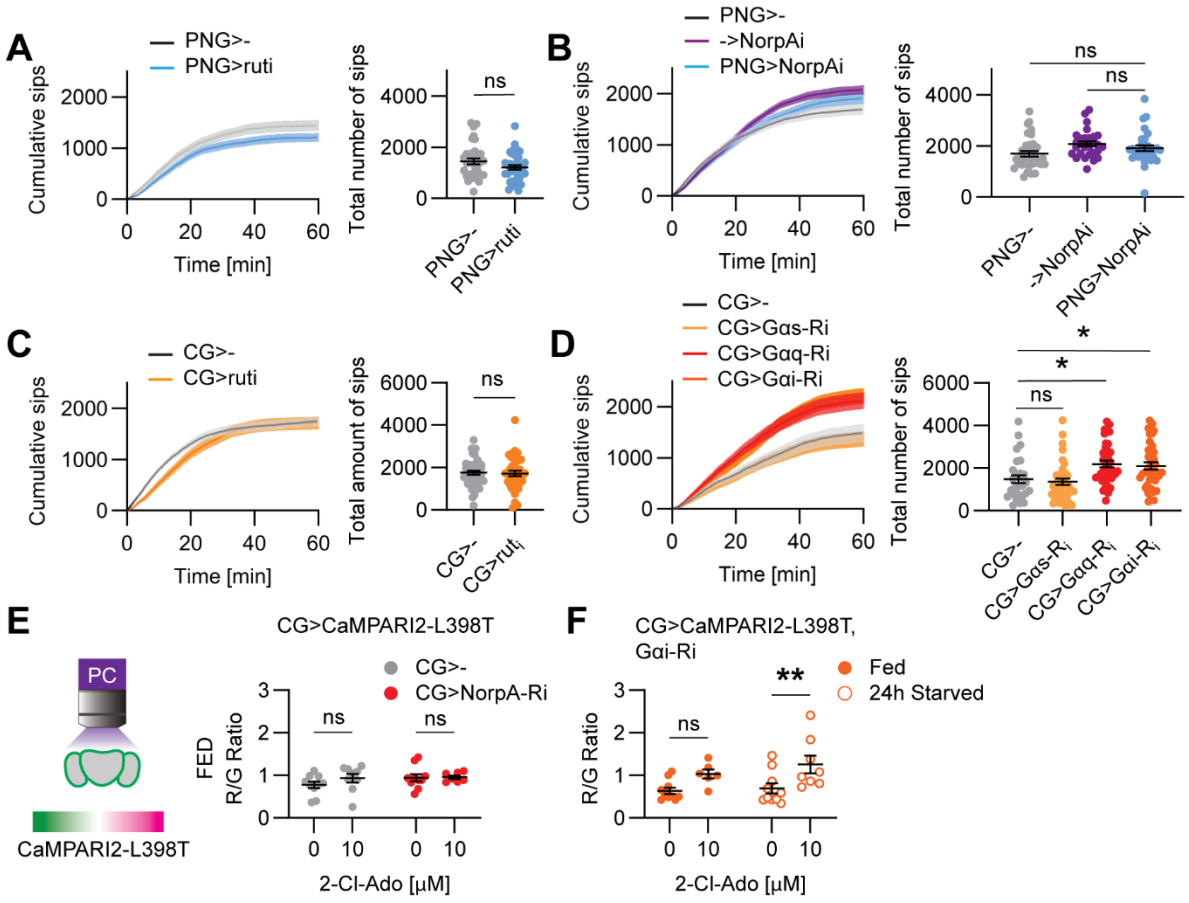

Figure S9: Adenosine signals hunger state through distinct pathways in astrocyte-like and in cortex glia (related to Figure 6)

(A) Cumulative number of sips (mean ± SEM) and scatter plot of the total number sips on 10% sucrose drops in 24-h-starved control flies (PNG>-) or upon knockdown of *rutabaga* in PNG (PNG>ruti; n = 36/40; Unpaired t test p = 0.09).

(B) Cumulative number of sips (mean ± SEM) and scatter plot of the total number sips on 10% sucrose drops in 24-h-starved control flies (PNG>- and ->NorpAi) or upon knockdown of NorpAi in PNG (PNG>NorpAi; n = 35/31/32; Kruskal-Wallis test p = 0.0043).

(C) Cumulative number of sips (mean ± SEM) and scatter plot of the total number sips on 10% sucrose drops in 24-h-starved control flies (CG>-) or upon knockdown of *rutabaga* in CG (CG>ruti; n = 45/39; Unpaired t test p = 0.82).

(D) Cumulative number of sips (mean ± SEM) and scatter plot of the total number sips on 10% sucrose drops in 24-h-starved control flies (CG>-) or upon knockdown of the Gα-proteins -s, -q and -i in CG (CG>Gαs-Ri, CG>Gαq-Ri and CG>Gαi-Ri; n = 30/40/38/40; Kruskal-Wallis test $p < 0.0001$).

(E) CaMPARI2 photoconversion ratios measured in explant brains from fed control flies (CG>-) or upon knockdown of *NorpA* in CG (CG>NorpAi). Before photoconversion, explant brains were kept for 10 minutes in saline solution containing or not 10 µM of 2-Cl-Ado (CG>- n = 10/9; Mann-Whitney test p(2-Cl-Ado) = 0.13; CG>NorpAi n = 10/7; Welch's t test p(2-Cl-Ado) = 0.91; CG>- vs. CG>NorpAi Unpaired t test p = 0.22).

(F) CaMPARI2 photoconversion ratios measured in explant brains from fed or 24-h-starved flies upon knockdown of Gαi in CG (CG> Gαi-Ri). Before photoconversion, explant brains were kept for 10 minutes

in saline solution containing or not 10 µM of 2-Cl-Ado (n_{Fed} = 10/6; $n_{Starved}$ = 10/8; 2-way ANOVA p(feeding state) = 0.31, p(2-Cl-Ado) = 0.0015, p(interaction) = 0.55).
Scatter plots display individual data points, as well as the mean ± SEM for each group. Post hoc pair-wise comparisons are indicated as follow: ns, non-significant ($p > 0.05$); *, $p < 0.05$; **, $p < 0.01$; *** $p < 0.001$.

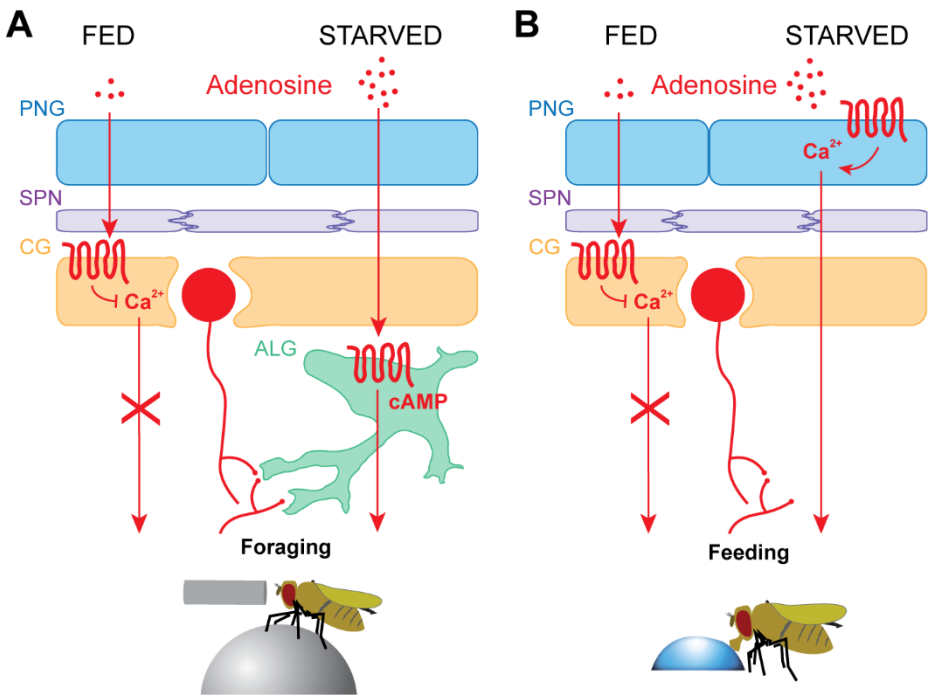

Figure S10: Summary model for the modulation of metabolic state-dependent behavior by adenosine signaling in glia

(A) Adenosine signaling prevents calcium increase in CG, refraining fed flies from tracking food-odor. In starved flies, increased extracellular adenosine concentration promotes cAMP-related signaling in ALG that in turn promotes food-odor tracking behavior (B) Adenosine signaling prevents calcium increase in CG, refraining fed flies from feeding. In starved flies, adenosine induces cytoplasmic calcium increase in PNG and promotes feeding behavior.